



Impact of hydrogeochemical processes and its evolution in controlling groundwater chemistry along the east coast of Tamil Nadu and Puducherry, India

Faizal Khan¹ · Srinivasamoorthy Krishnaraj¹ · Prakash Raja¹ · Gopinath Selvaraj² · Rabina Cheelil¹

Received: 17 April 2020 / Accepted: 17 September 2020 / Published online: 1 October 2020
© Springer-Verlag GmbH Germany, part of Springer Nature 2020

Abstract

The present study area falls beside the coastal zone of Tamil Nadu, and Puducherry is characterized by varied geological formations that mostly contain groundwater resources that are primarily utilized for domestic, agricultural, industrial, and other utilities. The study aims to differentiate various hydrogeochemical processes responsible for disparities in water chemistry. Groundwater samples were collected from 66 sites during the two major seasons: pre-monsoon and post-monsoon. The analytical data were separated into terrain vice and utilized for preparing graphical plots as well as mathematical calculations to obtain the existing relationship among chemical constituents and water quality. The Ca-HCO₃, Na-Cl, Ca-Na-HCO₃, mixed Ca-Mg-Cl, Ca-Cl, and Na-HCO₃ are the main hydrochemical facies observed from the groundwater samples. The ionic relationship among the samples indicates the control of direct and reverse ion exchange in the concentration of Ca²⁺, Mg²⁺, Na⁺, and K⁺ in groundwater. Moreover, silicate weathering contributes more in comparison with carbonate and evaporite dissolution. Gibbs plots reveal that water-rock interaction and evaporation processes are the main mechanisms controlling the water chemistry. The saturation index of different mineral phases indicates groundwater to be oversaturated with silicate mineral phases irrespective of the terrain. Statistical methods like correlation and principal component analysis were also performed to differentiate the specific association and possible source of the dissolved constituent in the groundwater. The study concludes the influence of multiple processes such as silicate weathering, direct and reverse ion exchange, secondary dissolution, saline water intrusion, and anthropogenic sources as the main reasons responsible for variation in groundwater chemistry.

Keywords Ion exchange · Silicate weathering · Saturation index · Rock-water interaction · Tamil Nadu and Puducherry

Introduction

Groundwater plays a vital role in water supply for domestic purposes in both urban and rural areas and represents the most reliable, hygienic, and reasonable natural resource (Bovolo et al. 2009). It plays a significant role in agricultural growth, especially in regions with semi-arid to arid climatic environments where the availability of surface water bodies is rare. In

such cases, intensive exploitation of groundwater systems is made to fulfil the emerging needs. Several aquifer systems around the world are not suitable concerning quality due to the influence of natural as well as anthropogenic activities (Kattan 2018). The quality of groundwater is directly related to the social and economic development of an area due to its substantial consequence over human health and agriculture. Rural areas with undesirable groundwater conditions may reduce the economy and restrain the living circumstances. In a global scale, groundwater delivers 25 to 40% of total drinking water (Morris et al. 2003); in India, it accounts for 88% (Jain et al. 2009).

Rapid urbanization and population growth make coastal ecosystems to suffer human disturbances (Sajil Kumar 2016). Groundwater is the safest source for drinking and domestic purpose in comparison with other surface water bodies. In coastal aquifers, groundwater and seawater are connected naturally by an interface; denser saline water stays at the

Responsible editor: Philippe Garrigues

✉ Faizal Khan
geofaizal@gmail.com

¹ Department of Earth Sciences, Pondicherry University, Pondicherry, India

² Instituto de Geofísica, Universidad Nacional Autónoma de México, Ciudad Universitaria, México, México City, México

bottom, whereas lighter freshwater remains floated over seawater. The contact between freshwater and seawater can be an abrupt one, termed as a sharp interface. In some cases, the connection may not be distinct and is in the form of a buffer zone with brackish water (Meadows et al. 2004; Buquet et al. 2016). The demand for groundwater is increasing exponentially due to the inadequate availability of alternate sources. The deficiency of alternative surface water sources triggers overexploitation of groundwater that leads to quality deterioration as well as water table decline.

The chemistry of underground water depends upon various factors such as weathering and dissolution of rock materials, nature of hydrogeochemical processes, the residence time of dissolved ions, and the nature of pollutants. Groundwater chemistry can provide a better understanding of hydrochemical characteristics, hydrochemical processes, and nature of the aquifer. It reflects the quality of groundwater and the prevailing environment of an area. Hydrochemical data are useful for monitoring the chemical change that takes place concerning space and time. It can give a clear picture of the processes and mechanism that has taken place along the course from recharge to discharge area. The variation of dissolved ion in water and their interrelationship may guide to probable sources of their origin and mechanism that altered the water chemistry. Salinity induced by the seawater is one of the significant threats for the coastal aquifer system in the world. Overdrafting of freshwater from the coastal aquifer is the vital cause for the inland movement of seawater. The salinization of coastal groundwater can be elucidated by different situations like low infiltration of freshwater, sea-level variations, hydraulic gradient along with the coast, and surplus withdrawal of coastal groundwater. Periodical analysis has to be done for accessing the salinization of coastal aquifers. Salinization of the coastal area may also happen due to human interference. It is essential to differentiate the sources of salinity and triggering processes.

Groundwater quality is highly influenced by geochemical processes and reactions that take place during rock-water interaction. These developments are accountable for the spatial and temporal disparities in water chemistry. The hydrochemical properties of groundwater are mainly based on the water chemistry in the recharge zone and hydrochemical processes that happen beneath the surface. Therefore, the quality of underground water along its course highly depends upon the physicochemical properties of aquifer material and its residence time along with anthropogenic activities in the terrain (Matthess 1982; Rajmohan and Elango 2003). Intense agricultural activities with the application of fertilizers and overdrafting of groundwater are some of the significant reasons for groundwater degradation, especially in rural areas (Batabyal and Gupta 2017). The spatial variation in recharge may also cause the concentration of solutes in groundwater (Schuh et al. 1997). After the monsoon, the rise

in the water table results in the dissolution of salts from the soil, increasing salts in groundwater.

Several attempts were made by researchers globally to establish the hydrochemical characteristics and their influence over groundwater chemistry. For example, Wen et al. (2005) studied the chemical components and salinity of groundwater from the Ejina Basin, China. The study finds out the dominance of silicate weathering and evaporation deposition in controlling the major ion chemistry. Batayneh et al. (2013) in the Gulf of Aqaba established the interaction between groundwater and seawater using major ion chemistry. The authors identified that the processes, such as mineral dissolution, weathering, evaporation, and residence time, have significantly controlled the groundwater chemistry. Zaidi et al. (2015) studied the groundwater from Saudi Arabia and concluded reverse ion exchange as the dominant process that controls the groundwater chemistry.

Another study made by Manjusree et al. (2017) identified the factors controlling the groundwater chemistry in the coastal zones of Kerala. The study reveals the chemistry groundwater is derived from weathering of carbonate and silicate minerals along with rock-water interaction. The research conducted by Sako et al. (2018) in Burkina Faso investigated the effect of hydrogeochemical processes and human activities on groundwater quality. The geochemical results were validated statistically and concluded the dominance of rock-water interaction over anthropogenic activity in controlling water chemistry. Substantial and comparable attempts made by opting hydrochemical methods to establish the groundwater characteristics in different areas are Rajmohan and Elango (2003), Kortatsi et al. (2007), Mondal et al. (2010b), Wirmvem et al. (2014), Adimalla et al. (2018), Kattan (2018), and Sunitha and Sudharshan Reddy (2019).

The study area falls along the east coast of Tamil Nadu covering coastal zones of Kancheepuram, Villupuram, and Puducherry. The area is characterized by the presence of Archean and sedimentary aquifers. The Archean aquifers occupy the inland, whereas sedimentary aquifers lie along the coast. The area is known for agricultural, industrial, aquaculture, and salt pan activities. As per the Central Ground Water Board (CGWB) record, the study area experiences high groundwater development irrespective of litho units. The groundwater development in Archean terrain is mainly by dug wells and dug cum bore wells. Here groundwater is the primary source for irrigation activities, and it is abstracted for various domestic and industrial routines. The average draft of groundwater from Archean formation is 1.20 ha m/year. In sedimentary terrain, the groundwater development is mainly through tube wells. The groundwater in sedimentary terrain is primarily used for agriculture, industrial, drinking, domestic aquaculture, and other routine purposes. The area also suffers waterlogging, industrial pollution, and seawater ingress along the coastal zones. Groundwater development towards the

central part of the study area is very high and exceeds 90%, and it is marked as a vulnerable zone for water table depletion (Central Ground Water Board (CGWB) 2009). In this scenario, the current study targets to evaluate the hydrogeochemical processes controlling groundwater and its evolution in varying lithological domains. A complete acquaintance of water quality, hydrochemical mechanisms, and sources of salinity is vital for groundwater management and sustainable growth in the future.

Study area

Description of the study area

The study area is situated along the Coromandel Coast of the Indian subcontinent. It lies as a linear patch of landmass along the east coast of Tamil Nadu, which possesses Kanchipuram, Villupuram district of Tamil Nadu, and the union territory of Puducherry (Fig. 1). The area falls between north latitude $11^{\circ} 52' - 12^{\circ} 38'$ and east longitudes $79^{\circ} 38' - 80^{\circ} 11'$ with an aerial extent of 1570 km^2 .

Climate, rainfall, and drainage

The area experiences a humid tropical climate with an average maximum and minimum temperature in the range of 23.9 to 32.7°C . The summer is marked between April and July, where the temperature reaches its maximum; it may hit up to 40°C . The area receives maximum rainfall during the northeast monsoon, which is set during the middle of December. The average annual rainfall received in the area is 1116.6 mm . The precipitation during northeast monsoon happens as cyclonic rain is triggered by low pressure in the Bay of Bengal. Palar River on the northern side and Gingee on the southern side are the major rivers draining the area. Gingee River joins the Bay of Bengal, forming two estuaries, viz. Chunnambar and Ariyankuppam, towards the south of the study area. The drainage pattern is sub-dendritic with low drainage density.

Geology

The area comprises two lithological domains, crystalline plutonic and sedimentary rocks. The crystalline plutonic rock consists of charnockites of Eastern Ghats Supergroup, occupied along the western part of the area. Sedimentary rock includes Gondwanas of Upper Jurassic to Lower Cretaceous, Ramanathapuram, Vanur sandstone, Ottai claystone, and Turuvai formation of Lower to Upper Cretaceous, Kadaperikuppam Manaveli formation of Palaeocene, Cuddalore formation of Mio-Pliocene, and unconsolidated coastal and aeolian sands of the modern age. Around 40% of

the study area is occupied by hard rock terrain, and the remaining 60% by sedimentary formation (Fig. 1).

Hydrogeological units

The northwestern and western parts of the area are composed of weathered and fissured crystalline formations, whereas sedimentary formations occupy the northeastern, eastern, and southern regions. The porous sedimentary structure occurs along the coastal side of the study area from north to south, which is represented by unconsolidated and semi-consolidated formations of Upper Jurassic to recent age. Sand layers of the unconsolidated alluvium form a potential aquifer system that occurs along the tiers of the Palar. The depth of the alluvium ranges between 6 and 12 m below ground level (bgl) with a specific yield ranging from 25.0 to $35.0 \text{ m}^3/\text{h}$. The infiltration wells with varying depth (5–12 m bgl) possess a yield of about $35 \text{ m}^3/\text{h}$.

Along with the coastal regions, windblown sand acts as an aquifer, where extraction of groundwater is by dug wells of shallow depth. The porous sedimentary formation in the study area is represented by semi-consolidated formations of Cretaceous and Tertiary age and unconsolidated formations of Quaternary age. Groundwater occurs under water table and confined conditions in these formations and is developed through dug wells, dug-cum-bore wells, and tube wells.

The consolidated formation of Archaean consists of fractured and weathered charnockites and gneiss. Groundwater occurrence in these formations is restricted with fractures and weathered residuum under semi-confined to unconfined and discontinuous conditions. Groundwaters in these zones are suitable for development through bore wells and dug wells constructed in fractures and intersection of fracture zones. The water level depth in fissured formation ranges from 3.50 to 8.34 m bgl and 1.32 to 7.53 m bgl during May 2006 and January 2007, respectively (Central Ground Water Board (CGWB) 2007a, b).

Materials and methods

Groundwater sampling and analysis

Groundwater samples were collected for two different seasons to decipher hydrochemical characteristics and evolution. The sampling was carried out during the year 2014, which represents post-monsoon (February 2014) and pre-monsoon (May 2014). Samples were collected in narrow-mouthed poly lab bottles, 1000 ml for significant ion analysis. Before sampling, the wells were subjected to 10 to 15 min pumping so that standing water in wells get removed. Bottles were filled with sample water without leaving any space for air bubbles. After sampling, the bottles were appropriately labelled and

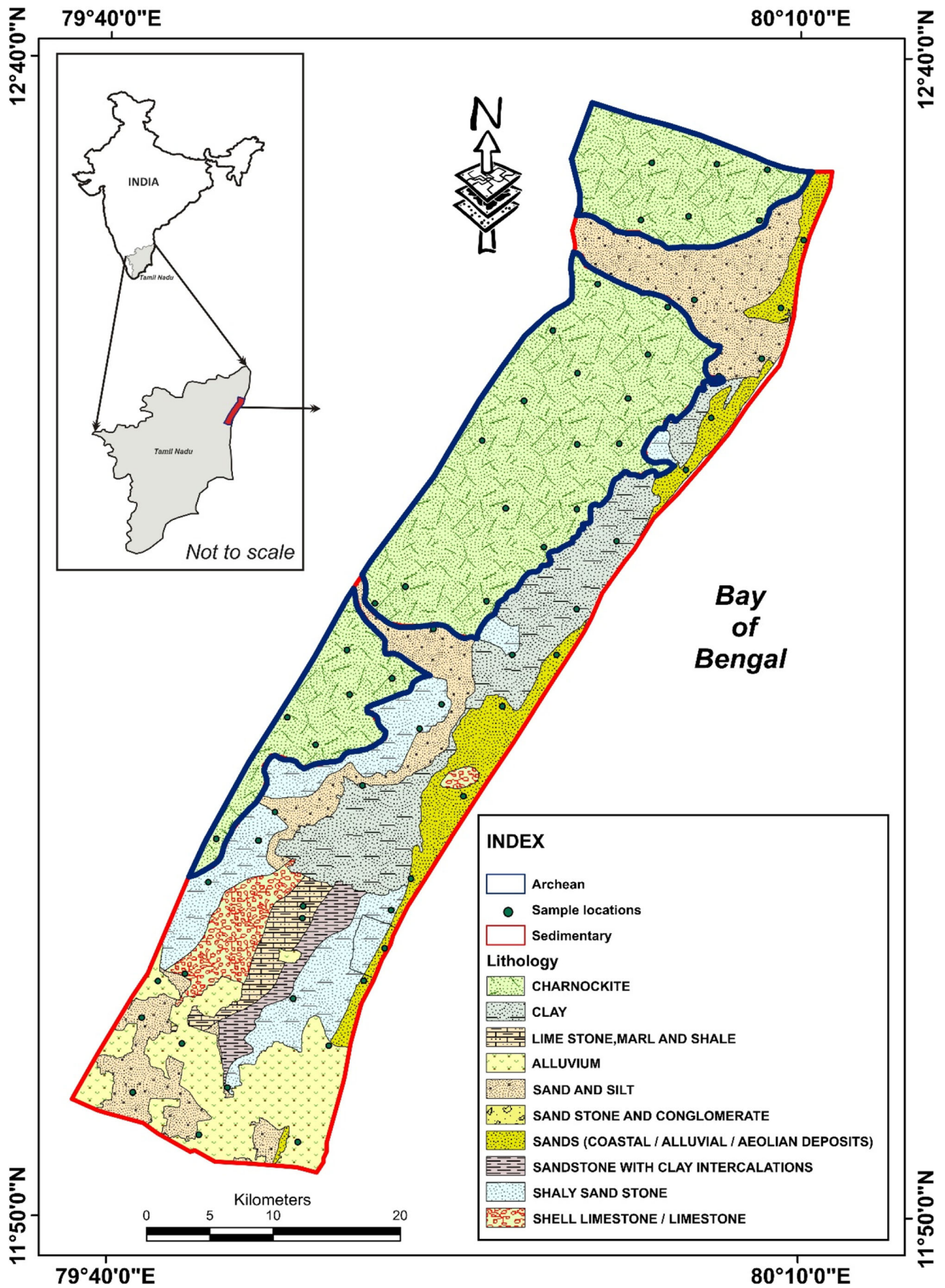


Fig. 1 Location map of the study area with geology and sample locations

transported carefully to Hydrogeology Laboratory, Department of Earth Sciences, Pondicherry University, and stored in 4 °C. The in-site parameters like pH, total dissolved solids (TDS), electrical conductivity (EC), and salinity were analysed in situ using a handy water quality analyser (PE 138). The cations like Ca^{2+} and Mg^{2+} were analysed by titration with standard EDTA solution. Anions, Cl^- and HCO_3^- , were determined by titration with HCL and AgNO_3^- . The univalent cations such as Na^+ and K^+ were estimated using a flame photometer (Systronics MK-I/MK-III). The dissolved silica is measured by the molybdosilicate method using a digital spectrophotometer (Elico SL 27). The SO_4^{2-} , PO_4^{3-} , NO_3^- , and F^- analyses were done by UV spectrometer (Elico SL-159) by adopting standard methods proposed by APHA (1995). Analytical precision has been checked using charge balance and TDS/EC ratio, which is well with the limit of 5 to 10%. The preparation of geological and location maps was performed in the ArcGIS version 10.2.1.

Hydrochemical facies and the evolution of groundwater are deciphered by piper trilinear diagram (Piper 1944). The hydrochemical relationships of dissolved chemical constituents in the groundwater are graphically represented in the piper diagram. The facies distribution and its nature can be studied along with insights of groundwater quality variation between and within aquifers (Srinivasamoorthy et al. 2014). The evaluation of hydrochemistry and facies evolution was attempted using major cations (Na^+ , Ca^{2+} , Mg^{2+} , and K^+) and anions (HCO_3^- , Cl^- , and SO_4^{2-}) concentration in meq/L. Chadha diagram is a modified form of piper diagram and extended Durov diagram with a significant difference in omitting triangular areas by Piper. Here the shape of the first study field is a rectangle or square based on the size of scale chosen for axes. The chemical data are plotted in milliequivalent percentage difference between $\text{Ca}^{2+} + \text{Mg}^{2+}$ (alkaline earth) and $\text{Na}^+ + \text{K}^+$ (alkali metal) in the x -axis and the difference between $\text{CO}_3^{2-} + \text{HCO}_3^-$ (weak acids ions) and $\text{Cl}^- + \text{HCO}_3^-$ (strong acid ions) in the y -axis.

The solubility of mineral phases in groundwater samples was determined using a computer-generated program PHREEQC code. Saturation index (SI) implies whether a mineral gets dissolved or precipitated in the water. SI is calculated using the given expression:

$$SI = \log (\text{IAP}/\text{KT})$$

Here, IAP stands for ion activity product and KT for solubility constant. When $SI = 0$, which indicates that water is in equilibrium, $SI > 1$ implies oversaturation, and $SI < 1$ denotes undersaturation.

Statistical treatment can decrease the mathematical difficulty of data and deliver substantial interpretation. The specific associations among the dissolved ions in water and their dispersal can be easily recognized by means of statistical

analysis. The statistical analysis for the present study has been done with the aid of the SPSS software. Correlation coefficient r is the resultant of correlation study; its value varies from -1 to $+1$. When r equals to $+1$, it indicates that variables have a perfect linear relationship in a positive manner, while r equals to -1 indicates a negative linear association among variables. When r value is 0, it implies no linear relationship between variables. The principle component analysis (PCA) was performed to the groundwater samples to evaluate the hydrochemical relationship among dissolved constituents and to estimate the chemical variables belonging to definite hydrochemical processes and their contribution towards the whole data sets. Factors with eigenvalues greater than or equal to 1 are taken into account. The statistical analysis extracted three factors Varimax rotated with Kaiser normalization for PRM and POM.

Results and discussions

Physicochemical parameters

Groundwater samples from Archean terrain show pH variations from 6.55 to 7.75 and 6.20 to 7.65 with averages of 7.15 and 6.97 during PRM and POM seasons, respectively. In sedimentary terrain, pH varies from 6.17 to 8.73 and 5.09 to 7.65 with an average of 7.10 and 6.67 in PRM and POM, correspondingly. Samples from both terrains show acidic to alkaline nature. The electrical conductivity of samples from Archean terrain ranges from 209.00 to 5620.00 $\mu\text{S}/\text{cm}$ and 410.00 to 3330.00 $\mu\text{S}/\text{cm}$ with a mean of 1588.00 and 1610.00 $\mu\text{S}/\text{cm}$ during PRM and POM seasons, respectively. In sedimentary terrain, EC values vary from 102.00 to 8930.00 $\mu\text{S}/\text{cm}$ with an average of 1386.00 $\mu\text{S}/\text{cm}$ in PRM and 130.00 to 4350.00 $\mu\text{S}/\text{cm}$ with an average of 1351.00 $\mu\text{S}/\text{cm}$ during POM season. The TDS values of well located in the Archean formation vary from 110.00 to 2970.00 mg/L and 217.00 to 1760.00 mg/L with averages of 837.57 and 818.61 mg/L in PRM and POM, correspondingly. In sedimentary wells, TDS values range from 53.90 to 4710.00 mg/L and 110.00 to 1730.00 mg/L with averages of 731.64 and 667.45 mg/L during PRM and POM correspondingly. Saline sources like seawater, aquaculture, salt pans, and the infiltration of pollutants accredit the elevated EC and TDS values in the area (Gopinath et al. 2017; Khan et al. 2020).

Cations and anions

The analytical results of major ions in groundwater samples collected during different seasons were displayed as boxplots (Fig. 2 and Table 1). The order of abundance of cations is $\text{Na}^+ > \text{Ca}^{2+} > \text{K}^+ > \text{Mg}^{2+}$ irrespective of seasons. In Archean territory during PRM, the order of cation abundance followed the

order as $\text{Na}^+ > \text{Ca}^{2+} > \text{Mg}^{2+} > \text{K}^+$. The abundance of anions in groundwater is $\text{HCO}_3^- > \text{Cl}^- > \text{NO}_3^- > \text{PO}_4^{3-} > \text{SO}_4^{2-} > \text{F}^-$ during PRM season irrespective of terrain, and during POM, it follows the order of $\text{HCO}_3^- > \text{Cl}^- > \text{NO}_3^- > \text{SO}_4^{2-} > \text{F}^- > \text{PO}_4^{3-}$ in both terrains. Elevated values of Na^+ in Archean terrain are mainly due to silicate weathering and cation exchange, whereas in sedimentary terrain, other sources like seawater intrusion, sea salt sprays, and evaporite dissolution also contribute sodium in groundwater (Srinivasamoorthy et al. 2011; Batayneh et al. 2013; Gopinath et al. 2017). Higher Ca^{2+} is noted in wells from the Archean formation, which indicates the release of Ca^{2+} through weathering of silicate minerals in charnockites (Srinivasamoorthy et al. 2008). In sedimentary terrain, Ca^{2+} might have derived from the dissolution of dolomite, gypsum, and anhydrite minerals. The cation exchange may also enhance the concentration of calcium in groundwater. Industrial waste and improper sewage dumping may also contribute to the higher concentration of Ca^{2+} in groundwater (Subrahmanyam and Yadaiah 2001). Elevated values of Mg^{2+} were noted during pre-monsoon season from the Archean terrain, which is attributed by silicate weathering from the country rock (Srinivasamoorthy et al. 2008).

Bicarbonate values in samples reported its maximum from sedimentary terrain samples, which might have derived from silicate weathering and carbonate dissolution from the atmosphere (Obeidatt and Alawneh 2019). Higher values of chloride were reported from sedimentary terrain samples, which is attributed by saline water intrusion, dissolution of evaporites, and salt pan activities (Subba Rao 2008; Srinivasamoorthy et al. 2013). High sulphate reported from the sedimentary terrain during the PRM season might be due to the influence of seawater along the coastal zones (Srinivasamoorthy et al. 2013). Fluoride in the samples reported maximum from the Archean terrain during POM season indicates geogenic source (Moncaster et al. 2000). Higher concentrations of PO_4^{3-} were reported from the sedimentary terrain, which might be a result of agricultural activity (Kortatsi et al. 2007), whereas the elevated values of nitrate reported from the sedimentary terrain during PRM season indicates the intense application of fertilizers for agricultural purpose (Mantelin and Touraine 2004).

Hydrochemical classification

The piper diagram consists of three distinct fields, diamond fields in the centre and two triangular in the lower left and right side of the diamond field. The concentrations of cations such as Mg^{2+} , Ca^{2+} , and $\text{Na}^+ + \text{K}^+$ are plotted in the left triangular field as a single point based on trilinear coordinates. Similarly, the concentrations of anions like HCO_3^- , Cl^- , and SO_4^{2-} are plotted in the right triangular field. These points are projected in the centre diamond field, where different fields

were marked. The water chemistry can be established from the diamond field.

In the piper diagram (Figs. 3 and 4), Archean and sedimentary terrain samples are plotted season-wise separately. In the Archean terrain, significant clusters were found in Ca-HCO₃, and Na-Cl field with minor representation is also noted in mixed Ca-Na-HCO₃, mixed Ca-Mg-Cl, Ca-Cl, and Na-HCO₃. Around 35 and 39% of samples from PRM and POM represent Ca-HCO₃ water type. The samples that fall in the Ca-HCO₃ field represents the recharge water with temporary hardness with more Ca^{2+} , Mg^{2+} , and HCO_3^- , which is out from the litho units through the filtration of water (Schoeller 1965). The Ca-Na-HCO₃ field samples specify the supremacy of ion exchange, which leads to permanent hardness (Playán and Mateos 2006). Na-Cl water type in the Archean terrain is represented by 28 and 7% of samples in PRM and POM season, separately. Sedimentary terrain samples cluster mainly in Na-Cl, Ca-HCO₃, Ca-Cl, and Na-HCO₃, and minor representations were also observed in mixed Ca-Na-HCO₃ and mixed Ca-Mg-Cl. Around 34% of the samples from sedimentary terrain irrespective of the season falls within the Na-Cl field, implying the influence of saline water intrusion along with the coastal areas. The Na-HCO₃-type water suggests the evolution of groundwater from Ca-HCO₃ through mixing, ion exchange evaporation, and prolonged interaction during the slow movement (Song et al. 2007). Samples that fall within the Ca-Cl field indicate the intermediate facies. As intrusion progresses, these facies further evolve along mixed Ca-Cl and mixed Na-Cl to reach Na-Cl facies that is closer to seawater (Mondal et al. 2010a; Srinivasamoorthy et al. 2011; Gopinath et al. 2019).

The new diagram proposed by Chadha (1999) for hydrochemical classification and hydrochemical process identification has also been attempted in the present study. Chadha's diagram for samples from different terrains in PRM and POM is displayed in Fig. 5. In the Archean terrain, 39% of samples irrespective of the season represents recharged water. This water type is characterized by the dominance of Ca^{2+} , Mg^{2+} , and HCO_3^- with temporary hardness. Around 25% each of the total samples during PRM season falls in field 6, and field 7 indicated reverse ion exchange and seawater. In the Archean terrain, field 7 represents the mature water with the dominance of Na^+ , Cl^- , and SO_4^{2-} . It points towards the anthropogenic activities in the study area. Minor representations were noted in field 8, indicating base ion exchange. Na^+ and K^+ ions from the aquifer material will get exchanged for Ca^{2+} and Mg^{2+} in groundwater (Zaidi et al. 2015). During POM, more representation was observed in reverse ion exchange and base ion exchange field, which indicates the influence of monsoon in rock-water interaction. In the sedimentary terrain, 39% and 25% of the samples represent the recharged water during PRM and POM seasons. About 21% and 46% of the samples fall with reverse ion

Table 1 Analytical results of physicochemical parameters in groundwater samples from the study area. All values are expressed in mg/L except pH and EC ($\mu\text{S}/\text{cm}$)

Parameters	Pre-monsoon (PRM)						Post-monsoon (POM)									
	Archean			Sedimentary			Archean			Sedimentary						
	Min	Max	Avg	Stdv	Min	Max	Avg	Stdv	Min	Max	Avg	Stdv	Min	Max	Avg	Stdv
pH	7.75	6.55	7.15	0.33	6.17	8.73	7.10	0.56	6.20	7.65	6.97	0.34	5.09	7.65	6.67	0.57
EC	5620.00	209.00	1588.29	1103.06	102.00	8930.00	1385.89	1526.52	410.00	3330.00	1610.43	803.81	130.00	4350.00	1351.11	978.58
TDS	2970.00	110.00	837.57	582.90	53.90	4710.00	731.64	804.56	217.00	1760.00	818.61	434.86	101.00	1730.00	667.45	403.23
Ca ²⁺	302.00	3.00	65.11	57.65	9.00	118.00	38.71	25.78	4.00	140.00	51.82	36.45	11.00	108.00	36.74	21.54
Mg ²⁺	128.00	5.00	31.27	25.31	2.40	76.80	22.59	18.91	6.00	68.00	27.61	12.86	5.00	87.00	20.85	14.65
Na ⁺	200.00	12.00	91.93	61.35	8.00	288.00	88.50	74.03	4.00	156.00	62.82	45.81	12.00	300.00	77.84	58.31
K ⁺	372.00	0.80	21.05	71.05	0.80	420.00	33.50	77.28	ND	355.00	29.82	86.61	ND	235.00	25.58	49.98
Cl ⁻	1395.00	40.00	252.80	286.87	15.00	2020.65	215.58	325.98	20.00	455.00	170.13	121.29	46.00	660.00	167.21	128.44
HCO ₃ ⁻	428.00	40.00	254.31	116.82	40.00	591.70	251.95	170.47	105.00	560.00	280.17	114.09	40.00	540.00	217.24	131.07
SO ₄ ²⁻	1.90	0.03	0.37	0.38	0.04	5.30	0.74	1.09	0.06	3.50	0.81	1.02	0.02	6.30	1.29	1.58
NO ₃ ⁻	32.50	0.20	9.13	8.92	0.50	82.50	14.45	17.85	0.20	32.50	4.19	6.87	ND	56.00	14.19	18.23
PO ₄ ³⁻	7.30	0.01	2.42	1.31	0.01	6.38	2.01	1.29	ND	2.75	0.19	0.59	ND	4.90	0.52	1.25
F ⁻	0.55	0.04	0.09	0.13	0.05	0.65	0.11	0.15	0.40	1.60	0.72	0.25	0.20	1.25	0.65	0.28
H ₄ SiO ₄	275.00	70.00	153.82	43.40	40.00	275.00	126.58	59.96	67.00	300.00	145.86	54.26	15.20	300.00	132.06	76.64

Max = maximum, Min = minimum, Avg = average, Stdv = standard deviation

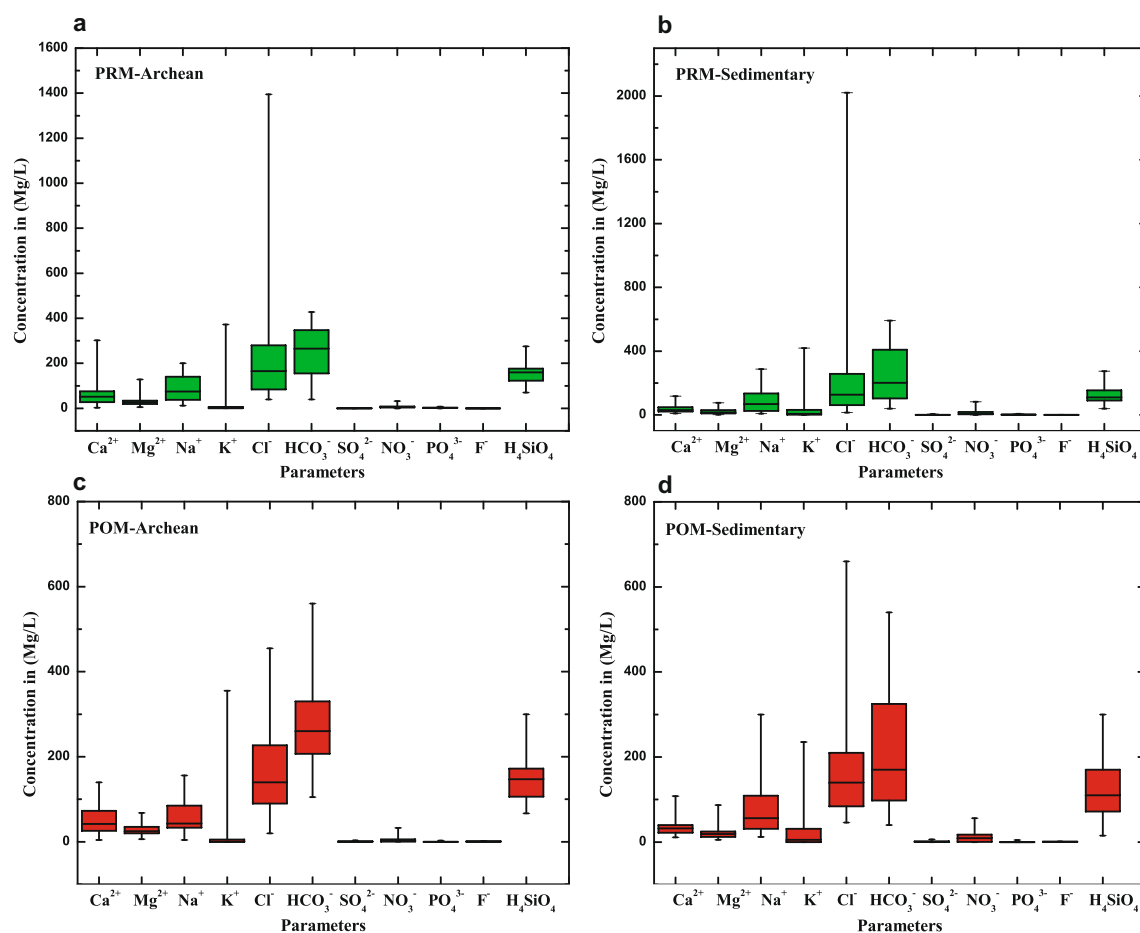


Fig. 2 Boxplots of major ion parameters in groundwater samples

exchange filed during the respective seasons. Approximately 25% and 17% of samples from PRM and POM season represent base ion exchange, whereas around 50% and 46% of the samples represent seawater during PRM and POM season, correspondingly. In the sedimentary terrain, reverse ion exchange is more significant in controlling the water chemistry, which leads to the development of Ca^{2+} and Mg^{2+} -dominant Cl^- water types or Cl^- -dominant Ca^{2+} and Mg^{2+} water types. The samples that fall with field 7 imply the salinization processes take place along the coastal zone, which leads to the development of Na-Cl and Na- SO_4 water types (Chadha 1999).

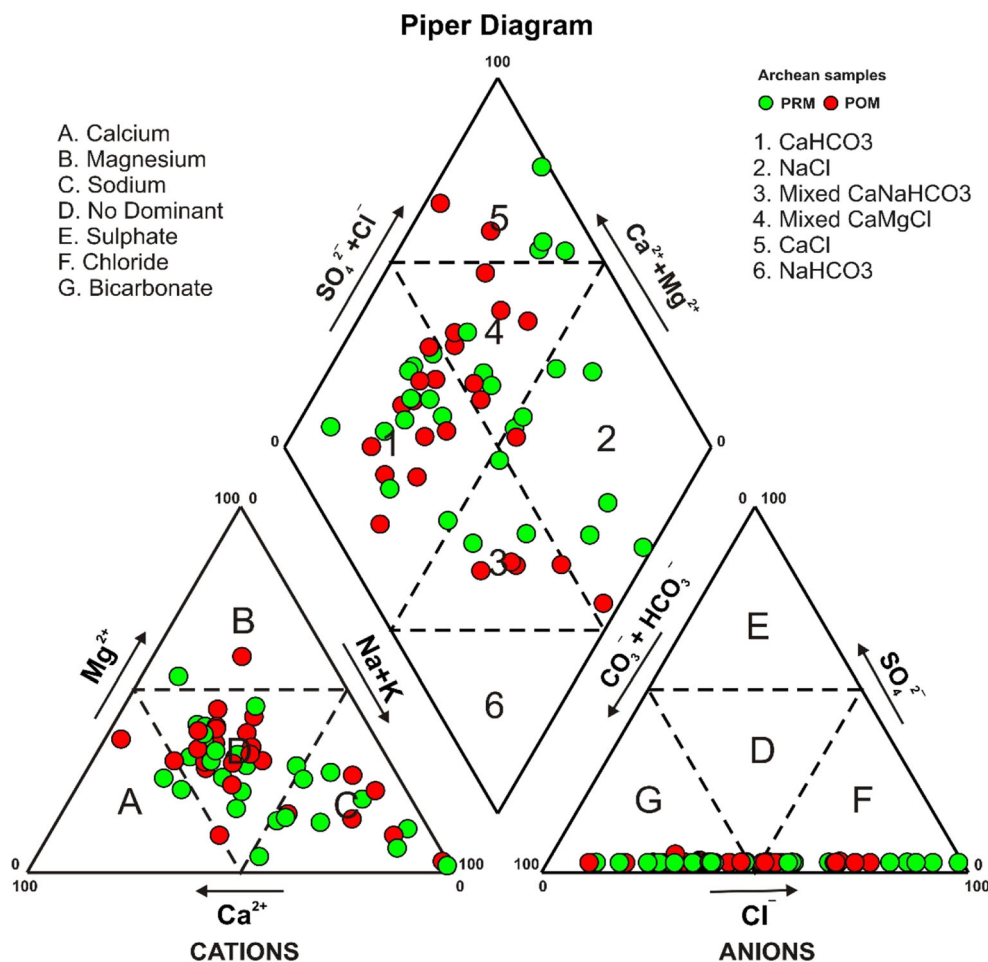
Processes controlling groundwater chemistry

The major hydrogeochemical processes that control the groundwater chemistry include ion exchange reaction, chemical weathering, evaporation, and anthropogenic activities. To establish the dominance of each method over water chemistry, hydrochemical, as well as statistical, techniques, were applied in the analytical data. The geochemical processes identified are discussed in detail in the subsequent subdivisions:

Silicate weathering

The three primary lithologies which undergo chemical weathering are carbonates, silicates, and evaporites (Garrels and MacKenzie 1971). Specific chemical signatures characterize groundwater draining through each lithology that depends upon the bedrock characteristics and rate of erosion. Generally, carbonate and evaporite rocks weather rapidly than granite rocks. The rate of weathering will be 12 times in carbonate rock and 40–80 times in evaporites (Meybeck 1987). The ratios of $\text{Ca}^{2+}/\text{Na}^+$, $\text{Mg}^{2+}/\text{Na}^+$, and $\text{HCO}_3^-/\text{Na}^+$ are more appropriate to differentiate silicates, carbonates, and evaporites and hold a unique property of the existing independent water fluxes and to the effects of evaporation (Gaillardet et al. 1997). The observed water types and chemical variation of ions propose a combination of different mechanisms in controlling the hydrochemical processes in the study area. The bivariate plot of Na^+ -normalized Ca^{2+} vs. Na^+ -normalized Mg^{2+} and HCO_3^- (Gaillardet et al. 1997; Mukherjee and Fryar 2008; Halim et al. 2010) is engaged in investigating the existence of silicate weathering, carbonate dissolution, and evaporation. The plots in Fig. 6 show that the best part

Fig. 3 Piper diagram for groundwater samples from the Archean terrain



of population represents silicate weathering field except for some samples which fall towards carbonate and evaporite dissolution field. It implies that silicate weathering is the main reason for the presence of Mg^{2+} and Ca^{2+} in the groundwater samples (Mapoma et al. 2017).

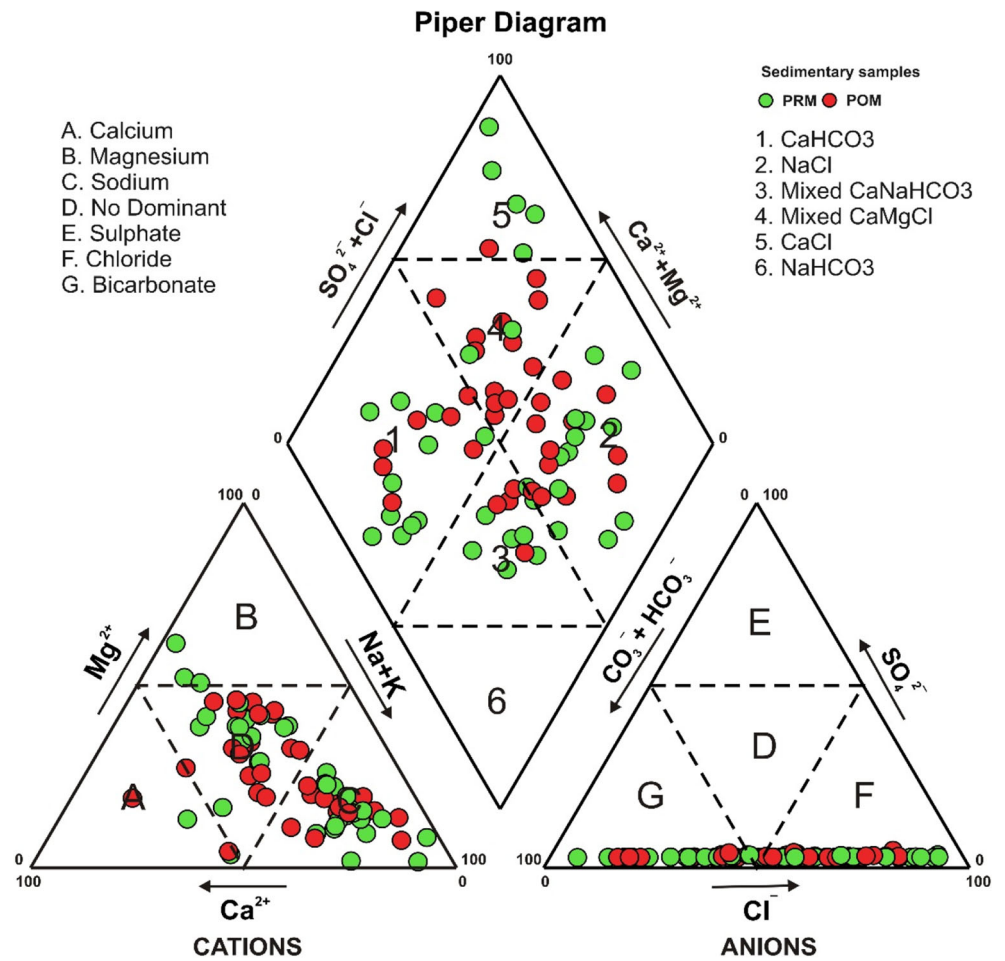
Ion exchange

The bivariate plot $(Na^+ + K^+) - Cl^-$ versus $(Ca^{2+} + Mg^{2+}) - (SO_4^{2-} + HCO_3^-)$ has been used to discriminate sources for Mg^{2+} and Ca^{2+} ions and in isolating cation exchange process (Fig. 7). The familiar additional sources of Ca^{2+} and Mg^{2+} include dissolution of gypsum, calcite, anhydrite, and dolomite other than cation exchange. Additional references are restricted by deducting SO_4^{2-} and HCO_3^- from the divalent cations (Ca^{2+} and Mg^{2+}) (Nkotagu 1996). Similarly, the same procedure is applied to Na^+ and K^+ to avoid the interference of silicate weathering and evaporite sources. In the plot, majority of the samples fall within the fourth quadrant (+ve ordinate and -ve abscissa), which indicates enrichment of Na^+ and K^+ concerning Ca^{2+} and Mg^{2+} . Sample plot within the second quadrant (-ve ordinates and +ve abscissa) indicates enrichment of Ca^{2+} and Mg^{2+} relative to Na^+ . The release of Mg^{2+}

and Ca^{2+} and absorption of Na^+ and K^+ during cationic exchange results in such enhancement (Yidana 2010; Monjerezi and Ngongondo 2012).

The bivariate plot of $Ca^{2+} + Mg^{2+}$ vs. $HCO_3^- + SO_4^{2-}$ can shed light upon the active geochemical processes in the study area. The sample poles will plot close to the equiline if Ca^{2+} , Mg^{2+} , HCO_3^- , and SO_4^{2-} are derived from the dissolution of dolomite, calcite, and gypsum. If the ion exchange reaction takes place, the samples will shift towards the right of equiline due to excess $HCO_3^- + SO_4^{2-}$ (Fisher and Mullican 1997), whereas the point shifts towards left due to reverse ion exchange with excess $Ca^{2+} + Mg^{2+}$. The plot shows that groundwater samples are spread on either side of the equiline irrespective of the terrain (Fig. 8). In the sedimentary terrain, more representation was observed close to equiline than the Archean terrain, indicating the dissolution of calcite, dolomite, and gypsum (Zaidi et al. 2015). The samples falling above and below equiline irrespective of the season suggest both mechanisms are responsible for controlling the groundwater chemistry of the study area. In Archean samples, the Ca^{2+} and Mg^{2+} are mainly due to the exchange of Na^+ in groundwater by Ca^{2+} and Mg^{2+} from aquifer materials. In such a case, the excess positive charge balance must be balanced by major anion Cl^- .

Fig. 4 Piper diagram for groundwater samples from the sedimentary terrain



The samples plotted below equiline are due to excess bicarbonate in groundwater. The excess negative charge due to $\text{HCO}_3^- + \text{SO}_4^{2-}$ must be balanced by only major cation Na^+ (Fisher and Mullican 1997).

The ion exchange reaction taking place between aquifer materials and groundwater during its interaction can be easily accessed by chloro-alkali indices CAI-1 and CAI-2 (Schoeller 1977). The CAI is calculated using the following expression:

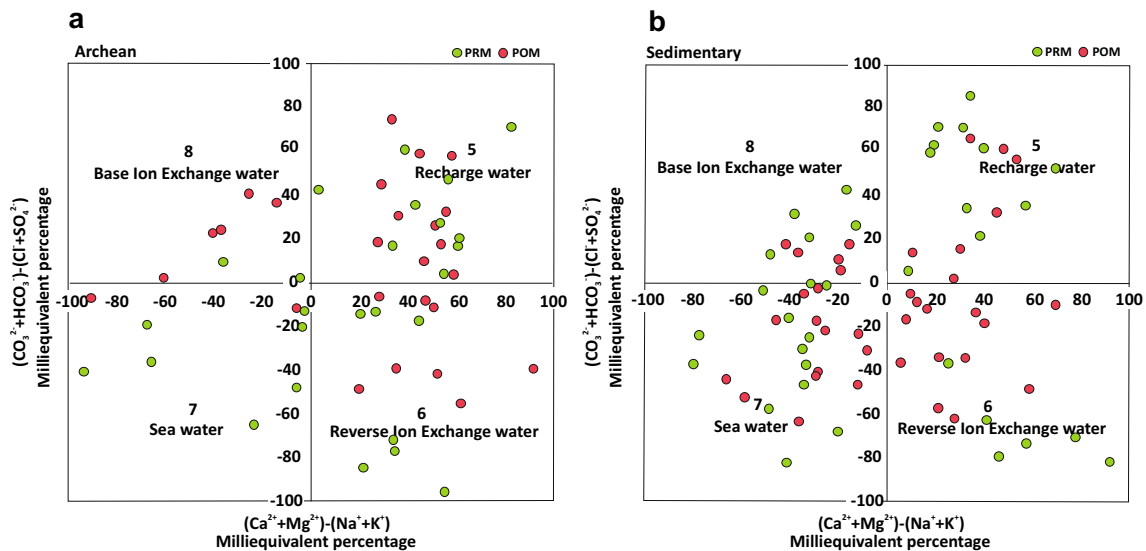


Fig. 5 Chadha diagram for groundwater samples

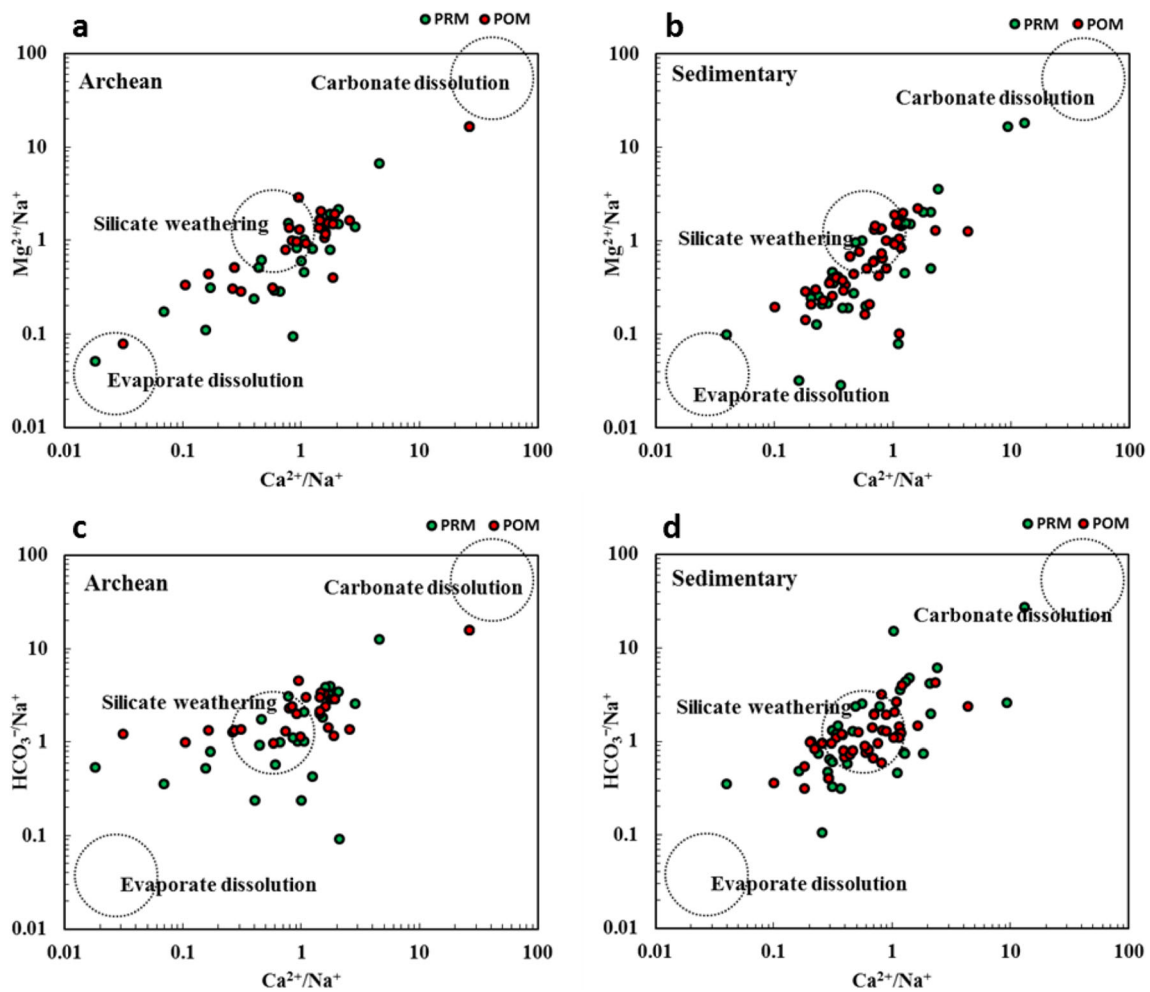


Fig. 6 Bivariate plot of (Mg^{2+}/Na^+) vs (Ca^{2+}/Na^+) and (HCO_3^-/Na^+) vs (Ca^{2+}/Na^+)

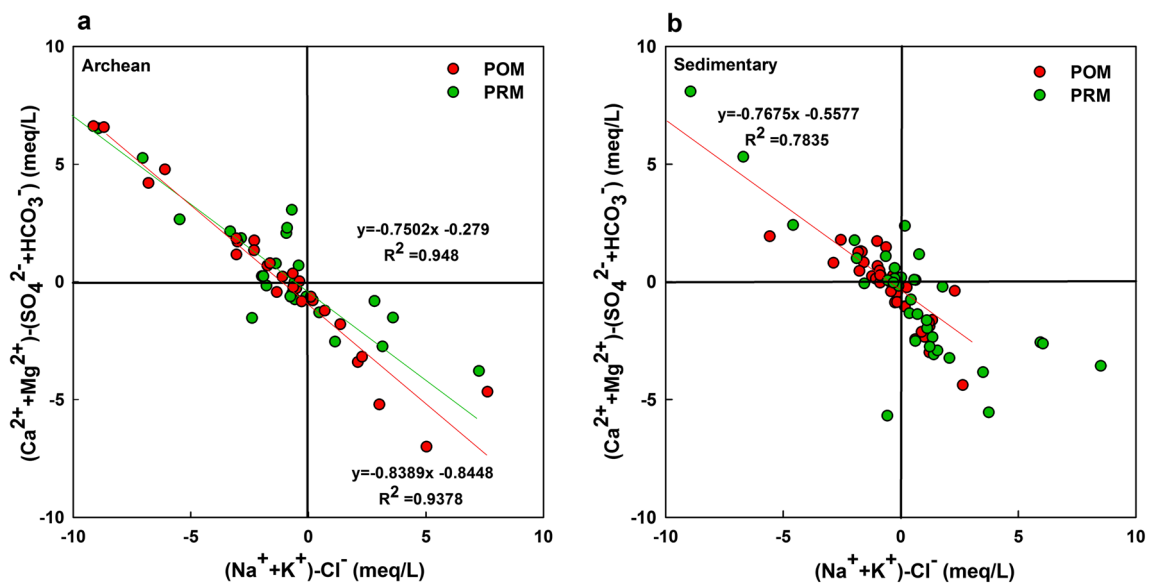


Fig. 7 Bivariate plot of $(Ca^{2+} + Mg^{2+}) - (SO_4^{2-} + HCO_3^-)$ vs $(Na^+ + K^+) - Cl^-$

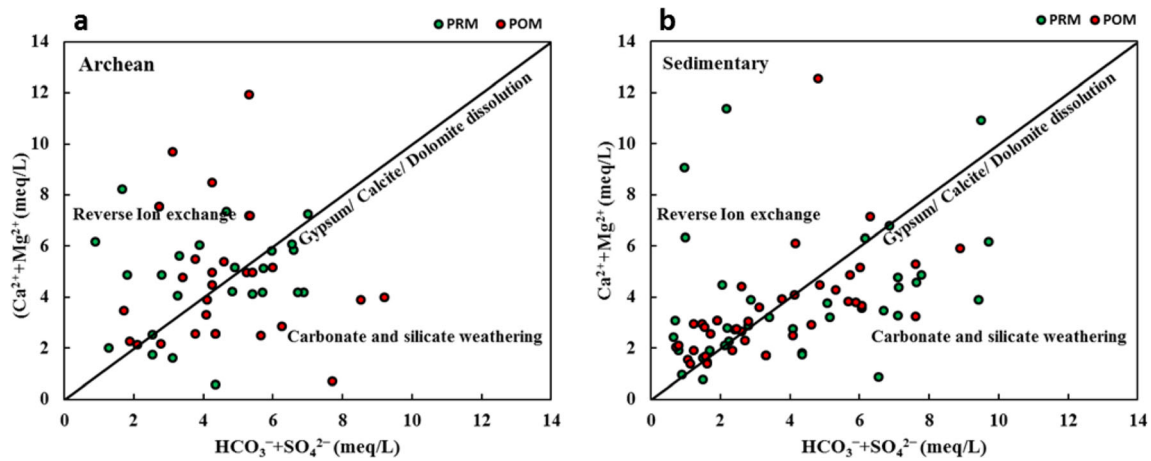


Fig. 8 Bivariate plot of $(Ca^{2+} + Mg^{2+})$ vs $(HCO_3^- + SO_4^{2-})$

$$CAI-I = \frac{(Cl^- - (Na^+ + K^+))}{Cl^-}$$

$$CAI-II = \frac{(Cl^- - (Na^+ + K^+))}{(SO_4^{2-} + HCO_3^- + CO_3^{2-} + NO_3^-)}$$

During reverse ion exchange, Na^+ and K^+ in groundwater will get exchanged for Ca^{2+} and Mg^{2+} in the aquifer material; the indices obtained will be positive, whereas the exchange of Ca^{2+} and Mg^{2+} in the water with Na^+ and K^+ in the aquifer material may happen during ion exchange and the resultant indices will be negative (Sako et al. 2018). From the plot (Fig. 9), the positive and negative indices of CAI indicate the part of both processes in controlling the hydrochemistry of the study area.

The mechanism controlling water chemistry

The genesis of groundwater and its quality is highly influenced by the interaction between aquifer materials and

groundwater (Cederstorm 1946). Gibbs (1970) has proposed a graphical representation of the natural processes that control water chemistry. According to him, the major processes which control water chemistry are evaporation, precipitation, and rock-water interaction. Separate plots were proposed for cations and anions. The Gibbs diagram for cations is prepared by putting the weight ratio of $Na^+ + K^+ / (Na^+ + K^+ + Ca^{2+})$ on the x-axis and TDS in the y-axis. For anions, the weight ration of $Cl^- / (Cl^- + HCO_3^-)$ is plotted against TDS on the y-axis. Gibbs plotted different water samples from the world in the diagram and obtained a curve with two arms. The first mechanism which controls water chemistry is atmospheric precipitation. The freshwater with low dissolved salts will only have salts supplied by precipitation. The data having precipitation dominance will be plotted on the right side of the lower arm. The second significant mechanism is rock-water interaction, for which the sources of dissolved salts are from aquifer materials (rock and soil). The groundwater that falls within this field is characterized by medium

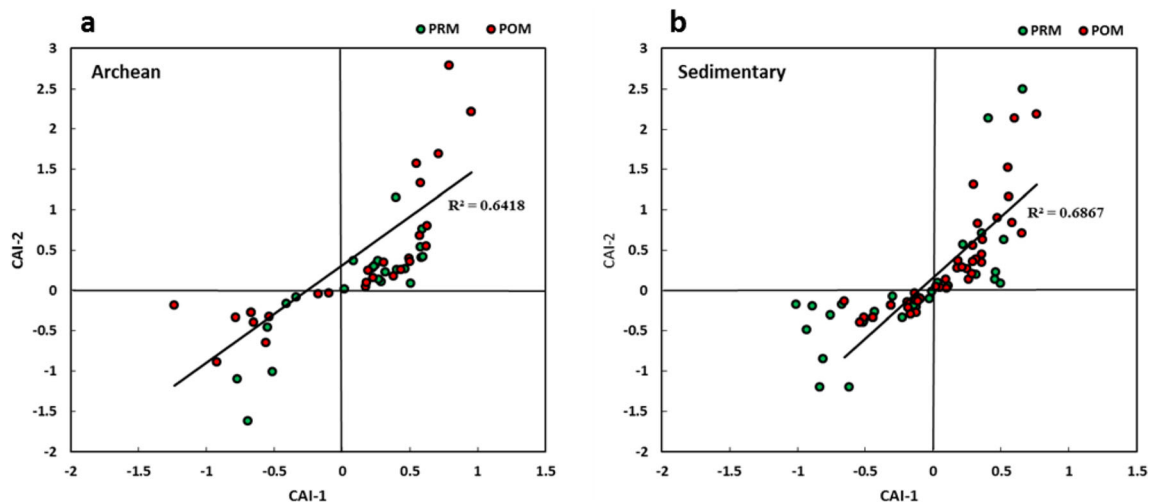


Fig. 9 Bivariate plot CAI-2 vs CAI-1

salinity with Ca^{2+} enrichment. Samples that falls within this field are in partial equilibrium with basin materials (Gibbs 1970). The third mechanism is the process of evaporation, which results in high saline Na-rich waters. The samples with evaporation dominance will fall towards the right side of the upper arm.

The Gibbs diagram for different terrains in PRM and POM is displayed in Fig. 10. In the Archean terrain, samples, irrespective of the season, which fall towards the middle of the rock dominance field imply the dissolution of Ca^{2+} and HCO_3^- from the aquifer materials during the course of the groundwater movement (Mondal et al. 2010b). Some of the samples that fall towards the right side of the rock dominance field indicate that the Na^+ and Cl^- show a deviation towards the right side of the upper arm, indicating the role of evaporation and concentration of salts in groundwater. In the sedimentary terrain, samples fall mainly in the rock dominance field with significant representation in the evaporation and precipitation fields. The precipitation dominance, water in the sedimentary terrain contains higher HCO_3^- and low dissolved salts, the considerable contribution of salts from atmospheric precipitation (Karanth 1989). The water tends to

move further towards rock dominance by prolonged interaction with the aquifer material; after that, the process of evaporation begins.

Saturation index

The hydrochemistry of groundwater is profoundly affected by solutes ensuing from the atmosphere, weathering, and dissolution of rock and soil materials. The interaction of groundwater with rock materials leads to mineral dissolution. During progressive dissolution, groundwater tends to saturate with a particular mineral at equilibrium condition. Furthermore, the dissolution of the same mineral leads to precipitation, and the water is said to be oversaturated with that mineral species. Calculation of groundwater saturation index helps to understand about the subsurface reactive minerals without solid-phase mineral analysis (Deutsch 1997). It is useful to find out the precipitated and dissolved minerals in water (Li et al. 2010).

The statistical summary of the saturation index of different mineral phases during PRM and POM is displayed in Table 2.

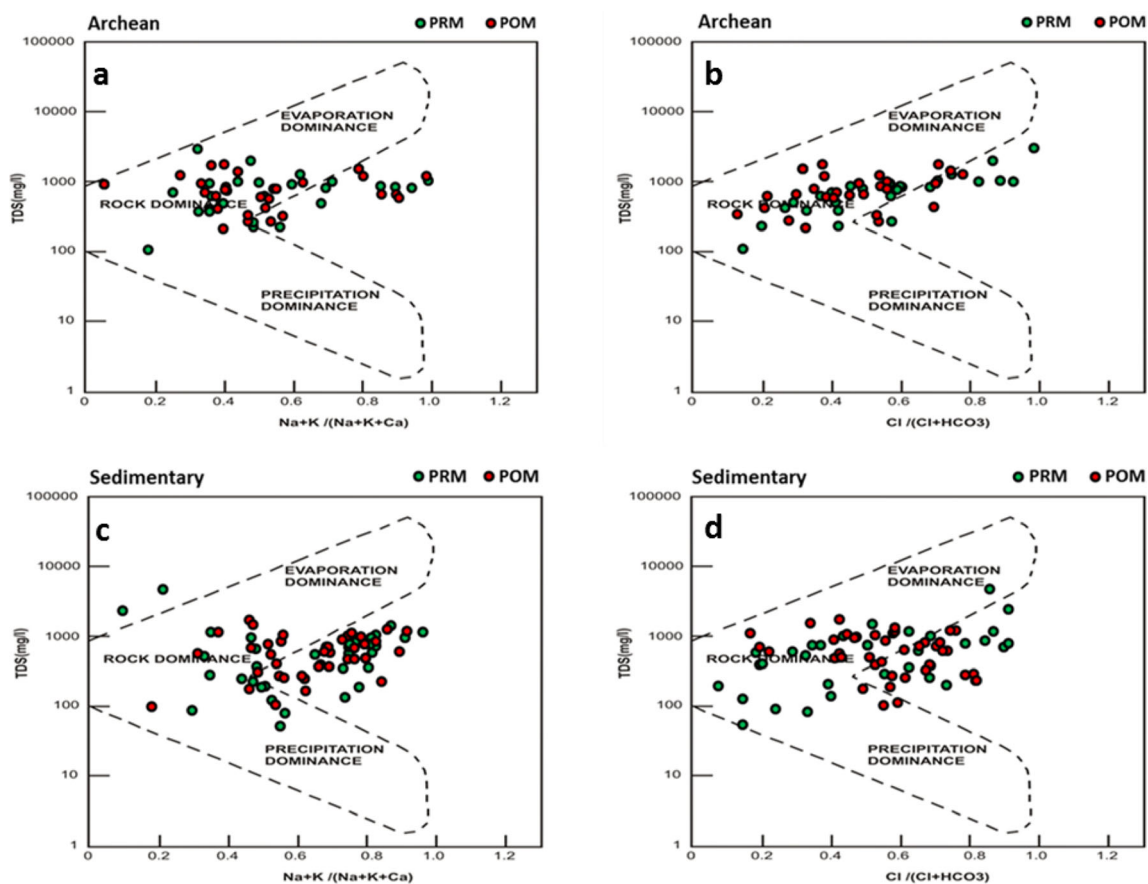


Fig. 10 Gibbs plots for groundwater samples

Table 2 Min, max, and average values of saturation indexes with respect to different mineral phases during PRM and POM

Mineral phase	Pre-monsoon—SI						Post-monsoon—SI					
	Archean			Sedimentary			Archean			Sedimentary		
	Min	Max	Avg	Min	Max	Avg	Min	Max	Avg	Min	Max	Avg
Anhydrite (CaSO ₄)	-5.77	-3.17	-4.63	-5.89	-3.47	-4.67	-5.51	-3.24	-4.49	-5.83	-2.95	-4.45
Aragonite (CaCO ₃)	-2.34	0.18	-0.74	-1.81	0.63	-0.44	-1.91	-0.04	-0.57	-3.37	-0.06	-1.11
Calcite (CaCO ₃)	-2.20	0.32	-0.60	-1.67	0.77	-0.30	-1.76	0.11	-0.42	-3.22	0.08	-0.97
Chalcedony (SiO ₂)	-1.53	1.05	-0.09	-0.63	1.21	0.46	0.60	1.25	0.92	-0.05	1.25	0.82
Chrysotile (Mg ₃ Si ₂ O ₅ (OH) ₄)	-13.84	0.10	-7.02	-12.17	-0.24	-5.34	-10.17	-1.39	-5.14	-17.76	-0.78	-7.65
Dolomite (CaMg(CO ₃) ₂)	-4.40	0.84	-1.12	-3.66	1.65	-0.55	-3.26	0.59	-0.69	-6.31	0.49	-1.85
Fluorite (CaF ₂)	-4.52	-1.86	-3.56	-4.88	-1.61	-3.67	-2.58	-1.09	-1.64	-3.04	-0.77	-1.83
Gypsum (CaSO ₄ ·2H ₂ O)	-5.55	-2.95	-4.41	-5.67	-3.25	-4.45	-5.29	-3.02	-4.27	-5.61	-2.73	-4.23
Halite (NaCl)	-8.28	-5.74	-6.63	-8.00	-5.30	-6.65	-7.86	-5.94	-6.77	-7.75	-5.33	-6.68
Quartz (SiO ₂)	-1.10	1.48	0.34	-0.20	1.64	0.89	1.03	1.68	1.35	0.38	1.68	1.25
Sepiolite (Mg ₂ Si ₃ O ₇ ·5OH·3H ₂ O)	-10.54	-0.84	-5.04	-9.20	0.85	-3.01	-5.36	0.46	-2.11	-10.94	1.35	-3.94
Sepiolite (d) (Mg ₂ Si ₃ O ₇ ·5OH·3H ₂ O)	-13.44	-3.74	-7.94	-12.10	-2.05	-5.91	-8.26	-2.44	-5.01	-13.84	-1.55	-6.84
SiO ₂ (a) (SiO ₂)	-2.37	0.21	-0.93	-1.47	0.37	-0.38	-0.24	0.41	0.08	-0.88	0.41	-0.02
Talc (Mg ₃ Si ₄ O ₁₀ (OH) ₂)	-11.28	2.97	-3.50	-9.53	4.93	-0.72	-4.51	4.16	0.40	-12.73	5.42	-2.31

Max = maximum, Min = minimum, Avg = average, SI = saturation index

Silicate mineral phases

The silicate mineral phases observed in the samples are quartz (crystalline silica), chalcedony (cryptocrystalline), SiO₂ (a) (amorphous), and chrysotile. In general, majority of samples during POM season show the oversaturated condition of quartz chalcedony and amorphous silica, whereas during PRM season, some samples show undersaturation of these mineral phases (Fig. 11 and Table 2). Chrysotile mineral phase shows undersaturated conditions during both seasons, irrespective of the terrain. The oversaturated state of mineral phases denotes the excess availability and prolonged interaction with groundwater, and under the saturated condition of chrysotile, it indicates limited availability. The continued interaction with groundwater and silicate minerals in the study area leads to the dissolution of silica in groundwater. The silica dissolution in groundwater is involved, which mainly depends upon the destructive nature of the solution. Silicate weathering triggers an intensification in pH by the consumption of acids (Appelo and Postma 2005). The pH and temperature of solution have more considerable influence over the dissolution of silicate mineral phases.

Carbonate mineral phases

The saturation indexes of carbonate minerals like calcite, dolomite, and aragonite were calculated and displayed in Table 2. The samples with negative values of SI indicate

undersaturation as a result of dissolution. Groundwater samples from the Archean terrain are comparatively undersaturated concerning carbonate mineral phases, which suggests that groundwater will tend to dissolve more carbonate mineral phases present in aquifer material (Chidambaram et al. 2012).

Magnesium mineral phases

The magnesium mineral phase present in the groundwater is formed due to water-rock interface and ion exchange. The undersaturated state of minerals indicates the unavailability of minerals and non-reactive nature. Mineral phases of sepiolite and sepiolite (d) during POM season shows under saturated condition (Fig. 11 and Table 2). The oversaturated nature of talc during both seasons indicated the availability of the mineral in aquifer material (Srinivasamoorthy et al. 2008).

Sulphate mineral phases

The saturation indexes of sulphate mineral phases in groundwater samples from both terrains irrespective of the season are in undersaturated condition. The undersaturated terms of sulphate minerals indicate the limited availability of these minerals in the aquifer matrix (Chidambaram et al. 2011).

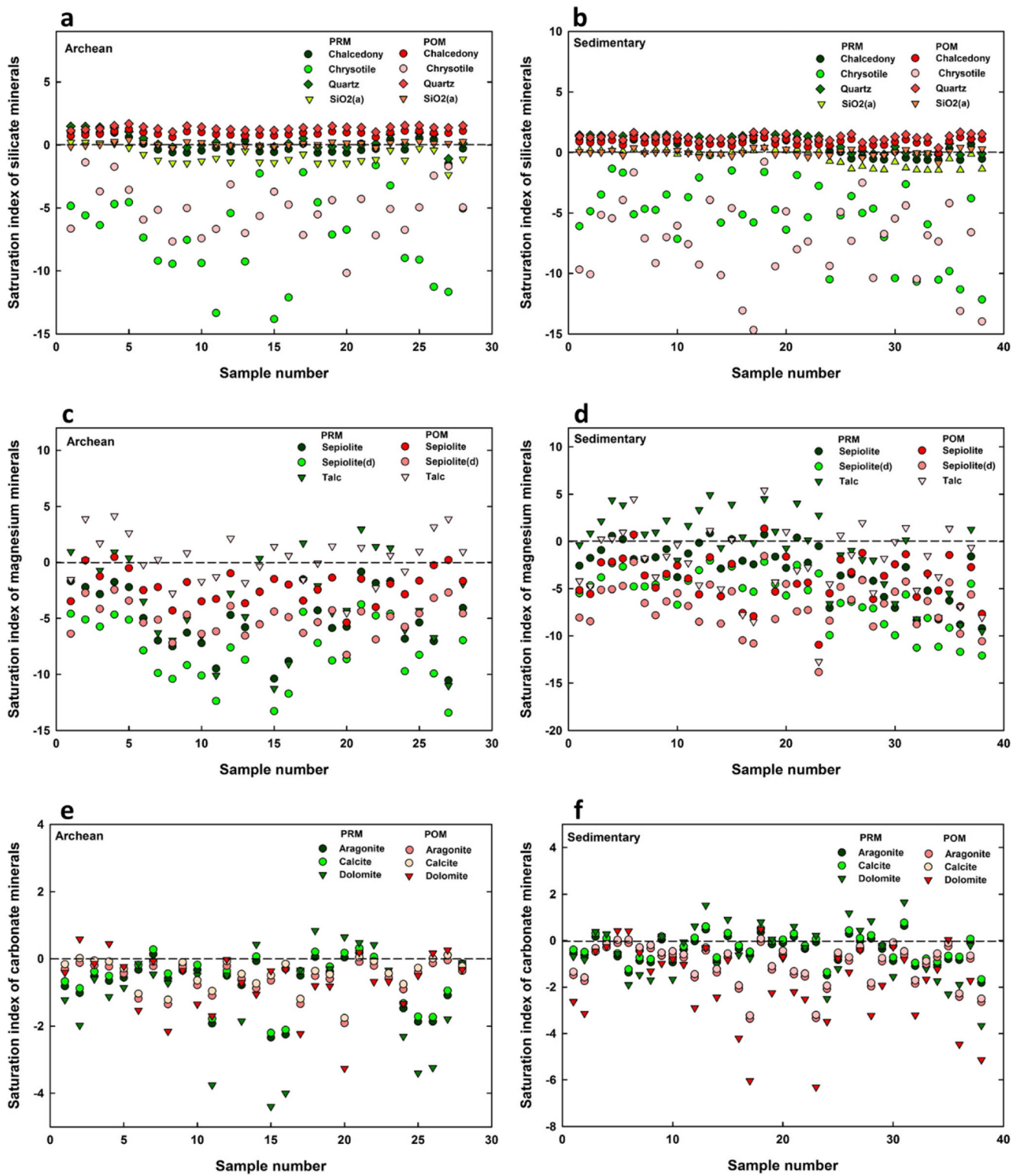


Fig. 11 Saturation indexes of various mineral phases

Table 3 Correlation matrix of groundwater sample from the Archean terrain during PRM

Parameter	pH	EC	TDS	Ca ²⁺	Mg ²⁺	Na ⁺	K ⁺	Cl ⁻	HCO ₃ ⁻	SO ₄ ²⁻	NO ₃ ⁻	PO ₄ ³⁻	F ⁻	H ₄ SiO ₄
pH	1													
EC	-0.44	1												
TDS	-0.43	0.99	1											
Ca ²⁺	-0.48	0.78	0.78	1										
Mg ²⁺	-0.45	0.72	0.72	0.88	1									
Na ⁺	-0.02	0.63	0.63	0.26	0.21	1								
K ⁺	0.16	0.08	0.08	-0.25	-0.24	0.37	1							
Cl ⁻	-0.42	0.91	0.91	0.89	0.82	0.58	0.07	1						
HCO ₃ ⁻	0.28	-0.38	-0.37	-0.29	-0.13	-0.14	-0.03	-0.42	1					
SO ₄ ²⁻	-0.27	0.68	0.68	0.60	0.62	0.58	0.00	0.72	-0.17	1				
NO ₃ ⁻	-0.05	0.19	0.19	-0.10	-0.09	0.12	-0.01	-0.04	0.02	0.01	1			
PO ₄ ³⁻	-0.01	0.21	0.21	0.19	0.06	0.33	0.22	0.32	-0.31	0.34	-0.04	1		
F ⁻	-0.21	0.19	0.20	-0.09	0.01	-0.15	-0.05	-0.12	0.09	-0.16	0.23	-0.52	1	
H ₄ SiO ₄	0.05	-0.21	-0.21	0.00	-0.16	-0.15	0.04	-0.07	0.07	-0.08	-0.15	-0.14	-0.28	1

*Values in bold indicate a significant relationship

Statistical analysis

Pearson correlation

The correlation analysis is a standard statistical technique in recognizing the relationship among two variables. The correlation matrix of various elements in groundwater during the different seasons is displayed in Tables 3, 4, 5, and 6. In the Archean terrain, PRM samples exhibit good positive correlation between EC and TDS ($r = 0.99$), Cl⁻ ($r = 0.91$), Ca²⁺ ($r = 0.78$), Mg²⁺ ($r = 0.72$), SO₄²⁻ ($r = 0.68$), and Na⁺ ($r = 0.63$). The high positive correlation among EC and TDS implies the absence of charged less-soluble compounds in groundwater

that may contribute to the total dissolved solids (Datta and Tyagi 1996). The positive correlation of other ions with EC and TDS implies their significant contribution to groundwater chemistry. A negative and weak positive correlation is observed between pH and other ions; this might be due to the highly destructive nature of the acidic medium, which leads to the concentration of certain ions. A significant high positive correlation with Cl⁻ and with other ions like Ca²⁺ ($r = 0.89$), Mg²⁺ ($r = 0.82$), SO₄²⁻ ($r = 0.72$), Na⁺ ($r = 0.58$), and NO₃⁻ ($r = 0.32$) may be due to secondary leaching of salts which were precipitated along with fractures, fissures, and other permeable zones in the Archean formation (Chidambaram et al. 2008). The correlation of SO₄²⁻ and NO₃⁻ indicates the

Table 4 Correlation matrix of groundwater sample from the Archean terrain during POM

Parameter	pH	EC	TDS	Ca ²⁺	Mg ²⁺	Na ⁺	K ⁺	Cl ⁻	HCO ₃ ⁻	SO ₄ ²⁻	NO ₃ ⁻	PO ₄ ³⁻	F ⁻	H ₄ SiO ₄
pH	1													
EC	-0.12	1												
TDS	-0.07	0.92	1											
Ca ²⁺	-0.37	0.53	0.44	1										
Mg ²⁺	-0.19	0.42	0.37	0.58	1									
Na ⁺	0.21	0.32	0.26	-0.10	-0.14	1								
K ⁺	-0.02	0.11	0.13	-0.17	-0.28	0.62	1							
Cl ⁻	-0.34	0.64	0.57	0.76	0.40	0.43	0.39	1						
HCO ₃ ⁻	0.36	0.33	0.25	-0.11	0.06	0.83	0.60	0.28	1					
SO ₄ ²⁻	-0.24	0.04	0.07	0.03	0.23	0.31	0.20	0.23	0.21	1				
NO ₃ ⁻	0.01	0.39	0.28	0.02	0.13	0.09	-0.14	-0.06	0.18	-0.08	1			
PO ₄ ³⁻	-0.06	0.16	0.19	0.05	0.02	0.49	0.36	0.25	0.53	0.20	-0.03	1		
F ⁻	0.45	0.05	0.02	-0.20	0.00	0.26	-0.09	-0.10	0.27	-0.06	-0.16	0.01	1	
H ₄ SiO ₄	-0.04	-0.02	0.06	-0.11	0.25	-0.17	-0.14	-0.19	0.10	-0.13	-0.06	-0.02	0.06	1

*Values in bold indicate a significant relationship

Table 5 Correlation matrix of groundwater sample from sedimentary rock terrain during PRM

Parameter	pH	EC	TDS	Ca ²⁺	Mg ²⁺	Na ⁺	K ⁺	Cl ⁻	HCO ₃ ⁻	SO ₄ ²⁻	NO ₃ ⁻	PO ₄ ³⁻	F ⁻	H ₄ SiO ₄
pH	1													
EC	-0.03	1												
TDS	-0.03	0.99	1											
Ca ²⁺	-0.05	0.56	0.57	1										
Mg ²⁺	0.12	0.69	0.69	0.57	1									
Na ⁺	-0.13	0.14	0.14	0.06	-0.13	1								
K ⁺	-0.17	0.21	0.21	0.07	0.04	0.41	1							
Cl ⁻	-0.09	0.93	0.93	0.52	0.61	0.65	0.16	1						
HCO ₃ ⁻	0.11	0.35	0.36	0.29	0.27	0.36	0.30	0.30	1					
SO ₄ ²⁻	-0.03	0.86	0.87	0.64	0.48	0.04	0.05	0.75	0.31	1				
NO ₃ ⁻	-0.11	0.11	0.10	-0.02	-0.17	0.38	0.28	0.01	-0.22	-0.04	1			
PO ₄ ³⁻	-0.08	0.50	0.50	0.37	0.31	0.20	0.52	0.48	0.37	0.35	0.30	1		
F ⁻	-0.31	-0.03	-0.03	-0.11	-0.01	0.04	-0.06	-0.02	-0.28	-0.05	0.21	-0.23	1	
H ₄ SiO ₄	-0.34	0.01	0.01	0.14	0.06	-0.02	-0.08	0.00	0.11	0.03	-0.21	0.03	0.10	1

*Values in bold indicate a significant relationship

influence of anthropogenic sources (Table 3). Archean samples during POM season shows that good to moderate positive correlations were obtained between Cl⁻ with EC ($r = 0.64$), TDS ($r = 0.57$), Ca²⁺ ($r = 0.76$), Mg²⁺ ($r = 0.40$), and Na⁺ ($r = 0.43$). Poor correlation of K⁺ with other ions might be due to superior resistance of potassium ions towards weathering and strong association with clay particles. A strong relationship between HCO₃⁻ and Na⁺ was also observed during the POM season, which indicates that both ions are the resultant of silicate weathering. The association of Ca²⁺ and Mg²⁺ signifies cation exchange and contribution of these ions towards the hardness of groundwater (Table 4). The moderate positive

correlation between Na⁺ and K⁺ indicates reverse ion exchange and enrichment of ions in groundwater (Sako et al. 2018). The significant positive relationship between K⁺ and Cl⁻ suggests the application of KCl fertilizers, which can also contribute K⁺ and Cl⁻ into groundwater (Lee et al. 2005).

In the sedimentary terrain during the PRM season, a high positive correlation is established between EC with TDS ($r = 0.99$), Cl⁻ ($r = 0.93$), SO₄²⁻ ($r = 0.86$), Mg²⁺ ($r = 0.69$), Na⁺ ($r = 0.63$), Ca²⁺ ($r = 0.56$), and PO₄³⁻ ($r = 0.50$). It indicates a significant contribution of these ions to groundwater chemistry. The moderate positive correlation between Ca²⁺ and Mg²⁺ implies cation exchange with aquifer materials under saline

Table 6 Correlation matrix of groundwater sample from sedimentary rock terrain during POM

Parameter	pH	EC	TDS	Ca ²⁺	Mg ²⁺	Na ⁺	K ⁺	Cl ⁻	HCO ₃ ⁻	SO ₄ ²⁻	NO ₃ ⁻	PO ₄ ³⁻	F ⁻	H ₄ SiO ₄
pH	1													
EC	0.19	1												
TDS	0.16	0.35	1											
Ca ²⁺	0.24	0.48	0.36	1										
Mg ²⁺	0.29	0.57	0.17	0.59	1									
Na ⁺	0.19	0.85	0.22	0.17	0.25	1								
K ⁺	-0.10	0.45	0.08	0.09	0.02	0.28	1							
Cl ⁻	0.10	0.92	0.13	0.44	0.58	0.80	0.34	1						
HCO ₃ ⁻	0.40	0.57	0.43	0.55	0.45	0.45	0.36	0.30	1					
SO ₄ ²⁻	-0.04	0.60	0.42	0.55	0.29	0.47	0.09	0.47	0.41	1				
NO ₃ ⁻	-0.19	0.39	0.24	-0.08	-0.12	0.31	0.74	0.25	0.09	0.16	1			
PO ₄ ³⁻	-0.01	0.25	0.06	0.16	0.00	0.12	0.63	0.16	0.33	0.09	0.49	1		
F ⁻	0.41	0.72	0.42	0.48	0.29	0.69	0.23	0.54	0.63	0.64	0.22	0.31	1	
H ₄ SiO ₄	-0.11	0.24	-0.08	0.15	0.24	0.23	-0.03	0.29	0.11	0.22	-0.10	0.18	0.23	1

*Values in bold indicate a significant relationship

Table 7 Principal component analysis of groundwater sample from the Archean terrain during PRM and POM

Parameters	Archean Pre-monsoon (PRM)				Archean Post-monsoon (POM)			
	Component			Communalities	Component			Communalities
	1	2	3		1	2	3	
pH	-0.48	0.46	-0.23	0.53	-0.25	0.05	0.81	0.74
EC	0.92	0.13	0.30	0.97	0.83	0.21	0.08	0.91
TDS	0.92	0.13	0.30	0.97	0.76	0.21	0.07	0.77
Ca ²⁺	0.90	-0.27	-0.15	0.93	0.86	-0.18	-0.24	0.85
Mg ²⁺	0.88	-0.28	-0.07	0.86	0.68	-0.12	-0.07	0.76
Na ⁺	0.54	0.70	0.11	0.81	0.13	0.87	0.27	0.88
K ⁺	-0.07	0.75	0.08	0.58	-0.06	0.80	-0.11	0.73
Cl ⁻	0.95	0.09	-0.03	0.96	0.82	0.36	-0.17	0.92
HCO ₃ ⁻	-0.22	0.16	-0.16	0.69	0.10	0.85	0.35	0.91
SO ₄ ²⁻	0.79	0.23	-0.10	0.69	0.12	0.45	-0.29	0.43
NO ₃ ⁻	-0.01	0.17	0.62	0.42	0.11	0.00	-0.09	0.81
PO ₄ ³⁻	0.15	0.35	-0.20	0.76	0.08	0.69	-0.08	0.51
F ⁻	0.03	-0.24	0.74	0.80	0.05	0.06	0.85	0.79
H ₄ SiO ₄	-0.06	0.00	-0.62	0.45	-0.08	-0.02	0.03	0.79
<i>Eigen value</i>	5.39	1.75	1.69		3.27	3.06	1.78	
<i>% variance</i>	38.53	12.47	12.05		23.33	21.84	12.74	
<i>Cumulative %</i>	38.53	51.00	63.04		23.33	45.17	57.91	

*Values in bold indicate a significant relationship

water intrusion (Jabal et al. 2014). The weak positive correlation between HCO₃⁻ with Ca²⁺, Mg²⁺, Na⁺, and K⁺ indicates the geogenic source (Jayakumar and Siraz 1997). A significant positive correlation between PO₄³⁻ and SO₄²⁻ indicates agricultural practices with the application of fertilizers (Table 5). The positive association among Na⁺ and Cl⁻ indicates the possibilities of saline water intrusion (Srinivasamoorthy et al. 2011). During the POM season, a strong relationship was observed between Na⁺-Cl⁻ ($r = 0.80$), Cl⁻-Mg²⁺ ($r = 0.58$), and Cl⁻-SO₄²⁻ ($r = 0.47$) suggests saline water intrusion along the coastal zones. The substantial positive relationship was also noted between ions like K⁺-PO₄³⁻ ($r = 0.63$), K⁺-NO₃⁻ ($r = 0.74$), and PO₄³⁻-NO₃⁻ ($r = 0.49$) which point towards the anthropogenic sources (Table 6).

Principle component analysis

The principle component analysis (PCA) of Archean samples during PRM extracted 3 factors with a total variance of 74.39%. Factor 1 displays 38.53% of the variance with strongly elevated loading of EC, TDS, Ca²⁺, Mg²⁺, Cl⁻, and SO₄²⁻ (Table 7). The higher loadings of Ca²⁺ and Mg²⁺ indicate cation exchange and silicate weathering. High loadings of Cl⁻ indicate the predominant leaching of salts from the upper soil horizon as a result of anthropogenic actions

(Srinivasamoorthy et al. 2008). Overexploitation of groundwater and upcoming of basal brine may also contribute excess Cl⁻ to groundwater. The specific loading of factor 1 also signifies the contribution of these ions towards EC and TDS. Factor 2 shows 12.47% of the variance with strong loadings of Na⁺ and K⁺, moderate loadings of pH, and PO₄³⁻. The positive loadings of Na⁺ indicate silicate weathering and ion exchange reactions. Na⁺ in groundwater may also derive from domestic wastes and the atmosphere (Edmunds et al. 2003; Brenot et al. 2008). Factor 3 with 12.05% of variance shows positive loading of NO₃⁻ and F⁻. The positive loadings of PO₄³⁻, NO₃⁻ and F⁻ imply the application of fertilizers and the influence of anthropogenic impact on groundwater chemistry. Since NO₃⁻ does not have any known geogenic source, it conforms to the domestic and industrial inputs (Handa 1988). During the POM season, PCA analysis of Archean samples extracted three factors with a total variance of 80.73%. Factor 1 with 23.33% of variance displayed strong positive loadings of EC, TDS, Ca²⁺, Mg²⁺, and Cl⁻ which conforms cation exchange, secondary leaching, and anthropogenic impacts in governing the groundwater chemistry of the study area (Table 7). Factor 2 displays 21.84% of the variance with strong loadings of Na⁺, K⁺, and HCO₃⁻ and moderate loading of PO₄³⁻. The typical loadings of Na⁺ and HCO₃⁻ indicate silicate weathering is the major source for Na⁺ in groundwater, which is confirmed by HCO₃⁻, the abundant

Table 8 Principal component analysis of groundwater sample from the sedimentary terrain during PRM and POM

Parameters	Sedimentary Pre-monsoon (PRM)				Sedimentary Post-monsoon (POM)			
	Component			Communalities	Component			Communalities
	1	2	3		1	2	3	
pH	- 0.01	- 0.24	0.43	0.71	0.13	- 0.11	0.03	0.86
EC	0.96	0.18	- 0.01	0.96	0.85	0.26	0.32	0.97
TDS	0.96	0.19	- 0.01	0.96	0.09	0.06	0.82	0.75
Ca ²⁺	0.70	0.04	0.15	0.54	0.10	0.04	0.63	0.78
Mg ²⁺	0.78	- 0.15	0.14	0.64	0.32	- 0.09	0.19	0.67
Na ⁺	0.76	0.13	0.00	0.58	0.93	0.11	0.13	0.91
K ⁺	0.07	0.80	0.10	0.65	0.24	0.89	0.01	0.86
Cl ⁻	0.91	0.12	- 0.02	0.85	0.87	0.13	0.09	0.90
HCO ₃ ⁻	0.30	0.38	0.67	0.72	0.22	0.32	0.51	0.76
SO ₄ ²⁻	0.88	0.03	0.03	0.77	0.44	- 0.02	0.73	0.81
NO ₃ ⁻	- 0.01	0.59	- 0.57	0.76	0.31	0.75	0.11	0.83
PO ₄ ³⁻	0.46	0.61	0.19	0.61	- 0.04	0.87	0.06	0.82
F ⁻	0.00	- 0.06	- 0.76	0.64	0.58	0.19	0.51	0.74
H ₄ SiO ₄	0.04	- 0.09	0.09	0.75	0.20	0.03	- 0.06	0.65
<i>Eigen value</i>	4.85	2.24	1.63		3.25	2.37	2.32	
<i>% variance</i>	34.67	16.01	11.65		23.22	16.92	16.55	
<i>Cumulative %</i>	34.67	50.68	62.33		23.22	40.13	56.68	

*Values in bold indicate a significant relationship

anion (Rogers 1989). Factor 3 with 12.74% of variance shows loadings of pH and F⁻, which implies the aggressive nature of the acidic medium in dissolving the ions.

The PCA of sedimentary terrain samples during PRM extracted three factors with a total variance of 67.313%. Factor 1 with 37.4% of variance shows higher loadings of EC, TDS, Mg²⁺, Ca²⁺, Na⁺, Cl⁻, and SO₄²⁻ which indicates the enhancement of salinity by mineral dissolution, ion exchange silicate weathering, secondary leaching, and saline water intrusion. Factor 2 explains a total variance of 17.3% with higher loadings of K⁺, NO₃⁻, and PO₄³⁻. The association of NO₃⁻ and PO₄³⁻ implies the role of human activities like the use of fertilizers and improper sewage disposal. Factor 3 accounts for 12.6% of the total variance and has higher loadings of pH and HCO₃⁻, which indicates the addition of H⁺ ions along with the HCO₃⁻ or might be due to the organic control over pH (Chidambaram et al. 2008; Vasanthavigar et al. 2012). During POM, factor 1 with 22.22% of variance shows loadings of EC, Na⁺, Mg²⁺, and Cl⁻ (Table 8). The high positive loadings of Na⁺ and Cl⁻ specify the possibilities of saline water intrusion along the coastal zone. Factor 2 exhibits a total variance of about 16.92% with elevated loading of K⁺, NO₃⁻, and PO₄³⁻, which once again confirms the anthropogenic impact over the water chemistry. The nitrate content of groundwater in the study might have derived from the domestic sewage effluents. Factor 3 with a total variance of 17.5% shows

higher loadings of TDS, Ca²⁺, SO₄²⁻, and F⁻, which directs the significant impact of these ions towards groundwater chemistry. The Ca²⁺ and F⁻ might be derived from geogenic sources, whereas SO₄²⁻ from saline water.

Conclusion

The study concludes the existence of multiple hydrochemical processes and various natural, as well as anthropogenic sources and controls the hydrochemistry in the study area. Ionic relationships of various ions refer to different mechanisms, and the causes that control the water chemistry are infiltration of recharge water, mineral dissolution, secondary leaching, ion exchange, silicate weathering, reverse ion exchange, anthropogenic sources, and saline water intrusion. Silicate weathering plays a significant role in releasing significant cations such as Ca²⁺, Mg²⁺, Na⁺, and K⁺ into the groundwater. Various ionic ratios indicate the existence of both direct and reverse ion exchange processes in controlling the concentration of ions. The hydrochemical facies shows an evolutionary trend from Ca-HCO₃ and Na-Cl fields via intermediate facies of mixed Ca-Na-HCO₃, mixed Ca-Mg-Cl, Ca-Cl, and Na-HCO₃. It implies the combined effect of various mechanisms like silicate weathering, ion exchange, subsequent dissolution, and human interferences over groundwater

chemistry. The Ca-HCO₃ type represents recharge water in the area; progressive evolution results in transformation to Na-Cl type, especially along the coastal zone with signatures of saline water intrusion.

The saturation index of groundwater samples shows silicate mineral phases like quartz and chalcedony in oversaturated conditions, and chrysotile shows undersaturated state irrespective of the terrain. In contrast, amorphous silica exhibits saturated to undersaturated condition regardless of terrain and seasons. The SI of carbonate minerals displays in Archean terrain; majority of the samples show undersaturated state except for few samples, which show saturated to oversaturated condition. In contrast, in sedimentary terrain, comparatively more samples show saturation to oversaturated status of carbonate mineral phases. The SI of magnesium mineral phase irrespective of terrain exhibits undersaturation of sepiolite and sepiolite (d) and saturated to oversaturated condition of the talc mineral phase. The SI of sulphate mineral shows undersaturated conditions irrespective of terrain and season. The Gibbs diagram specifies that rock-water interaction including dissolution and chemical weathering is the prime factor that controls the chemistry of groundwater. The correlation and factor analysis also points out the influence of various processes like secondary leaching of salts, silicate weathering, reverse ion exchange, anthropogenic sources, and saline water on controlling the water chemistry. The specific correlation between ions suggests multiple sources and mechanisms behind their occurrences. The PCA analysis reveals that groundwater chemistry in the Archean terrain is generally governed by secondary leaching and dissolution of salts, silicate weathering, ion exchange, and anthropogenic sources, whereas in the sedimentary terrain, factor 1 stands for the salinity and the ion exchange process, while factors 2 and 3 point out the influence of anthropogenic actions, use of fertilizers, improper sewage dumping, and domestic and industrial waste discharge over the groundwater chemistry.

Acknowledgements The author express his earnest gratitude towards the financing authority University Grants Commission for allocating (UGC)-BSR fellowship to accomplish the research.

Authors' contributions Faizal Khan: Data curation, performed writing—original draft

Srinivasamoorthy Krishnaraj: Conceptualization, visualization, writing, and reviewing and editing

Prakash Raja: Methodology, field work, software validation

Gopinath Selvaraj: Resources, investigation

Rabina Cheelil: Formal analysis

Funding The author express his earnest gratitude towards the financing authority University Grants Commission for allocating (UGC)-BSR fellowship to accomplish the research.

Data availability Not applicable.

Compliance with ethical standards

Conflict of interest The authors declare no conflict of interest.

Ethical approval Not applicable.

Consent to participate Not applicable.

Consent to publish Not applicable.

References

- Adimalla N, Li P, Venkatayogi S (2018) Hydrogeochemical evaluation of groundwater quality for drinking and irrigation purposes and integrated interpretation with water quality index studies. *Environ Process* 5(2):363–383. <https://doi.org/10.1007/s40710-018-0297-4>
- APHA (1995) Standard methods for the examination of water and wastewater (19th ed, p. 1467). Washington, DC
- Appelo CAJ, Postma D (2005) *Geochemistry, groundwater and pollution*, 2nd edn. Balkema, Rotterdam
- Batabyal AK, Gupta S (2017) Fluoride-contaminated groundwater of Birbhum district, West Bengal, India: interpretation of drinking and irrigation suitability and major geochemical processes using principal component analysis. *Environ Monit Assess* 189(8):369. <https://doi.org/10.1007/s10661-017-6041-0>
- Batayneh A, Zaman H, Zumlot T, Ghrefat H, Mogren S, Nazzal Y, Elawadi E, Qaisy S, Bahkaly I, Al-Taani A (2013) Hydrochemical facies and ionic ratios of the coastal groundwater aquifer of Saudi Gulf of Aqaba: implication for seawater intrusion. *J Coast Res* 30(1):75. <https://doi.org/10.2112/jcoastres-d-13-00021.1>
- Bovolo CI, Parkin G, Sophocleous M (2009) Groundwater resources, climate and vulnerability. *Environ Res Lett* 4(3):035001. <https://doi.org/10.1088/1748-9326/4/3/035001>
- Brenot A, Baran N, Petelet-Giraud E, Négrel P (2008) Interaction between different water bodies in a small catchment in the Paris basin (Brévilles, France): tracing of multiple Sr sources through Sr isotopes coupled with Mg/Sr and Ca/Sr ratios. *Appl Geochem* 23(1): 58–75. <https://doi.org/10.1016/j.apgeochem.2007.09.006>
- Buquet D, Sirieix C, Anschutz P, Malaurent P, Charbonnier C, Naessens F, Lecroart P (2016) Shape of the shallow aquifer at the fresh water–sea water interface on a high-energy sandy beach. *Estuar Coast Shelf Sci* 179:79–89. <https://doi.org/10.1016/j.ecss.2015.08.019>
- Cederstorm DJ (1946) Genesis of groundwater in the coastal plain of Virginia. *Environ Geol* 41:218–245
- Central Ground Water Board (CGWB), (2007a) District groundwater brochure Kancheepuram district. http://cgwb.gov.in/district_profile/tamilnadu/kancheepuram.pdf. Accessed 15 Oct 2017
- Central Ground Water Board (CGWB), (2007b). Groundwater brochure of Puducherry Region U.T of Puducherry, pp 1–27. http://www.cgwb.gov.in/District_Profile/Puduchery/Puducherry.pdf. Accessed 15 Oct 2017
- Central Ground Water Board (CGWB), (2009). District groundwater brochure Villupuram district, Tamil Nadu. Technical report series. http://cgwb.gov.in/district_profile/tamilnadu/villupuram.pdf. Accessed 15 Oct 2017
- Chadha DK (1999) A proposed new diagram for geochemical classification of natural waters and interpretation of chemical data. *Hydrogeol J* 7(5):431–439. <https://doi.org/10.1007/s100400050216>
- Chidambaram S, Senthil Kumar G, Prasanna MV, John Peter A, Ramanathan A, Srinivasamoorthy K (2008) A study on the hydrogeology and hydrogeochemistry of groundwater from different depths

- in a coastal aquifer: Annamalai Nagar, Tamilnadu, India. *Environ Geol* 57(1):59–73. <https://doi.org/10.1007/s00254-008-1282-4>
- Chidambaram S, Karmegam U, Sasidhar P, Prasanna MV, Manivannan R, Arunachalam S, Anandhan P (2011) Significance of saturation index of certain clay minerals in shallow coastal groundwater, in and around Kalpakkam, Tamil Nadu, India. *J Earth Syst Sci* 120(5):897–909. <https://doi.org/10.1007/s12040-011-0105-2>
- Chidambaram S, Prasanna MV, Singaraja C, Thilagavathi R, Pethaperumal S, Tirumalesh K (2012) Study on the saturation index of the carbonates in the groundwater using WATEQ4F, in layered coastal aquifers of Pondicherry. *J Geol Soc India* 80(6):813–824. <https://doi.org/10.1007/s12594-012-0210-0>
- Datta PS, Tyagi SK (1996) Major ion chemistry of groundwater in Delhi area: chemical weathering processes and groundwater flow regime. *J Geol Soc India* 47:179–188
- Deutsch WJ (1997) *Groundwater geochemistry: fundamentals and applications to contamination*. Lewis Publishers, New York
- Edmunds WM, Shand P, Hart P, Ward RS (2003) The natural (baseline) quality of groundwater: a UK pilot study. *Sci Total Environ* 310(1–3):25–35. [https://doi.org/10.1016/s0048-9697\(02\)00620-4](https://doi.org/10.1016/s0048-9697(02)00620-4)
- Fisher RS, Mullican WF III (1997) Hydrochemical Evolution of sodium-sulfate and sodium-chloride groundwater beneath the Northern Chihuahuan Desert, Trans-Pecos, Texas, USA. *Hydrogeol J* 5(2): 4–16. <https://doi.org/10.1007/s100400050102>
- Gaillardet J, Dupre B, Allegre CJ, Négrel P (1997) Chemical and physical denudation in the Amazon River Basin. *Chem Geol* 142(3–4):141–173. [https://doi.org/10.1016/s0009-2541\(97\)00074-0](https://doi.org/10.1016/s0009-2541(97)00074-0)
- Garrels RM, MacKenzie FT (1971) *Evolution of sedimentary rocks*. Norton, New York
- Gibbs RJ (1970) Mechanisms controlling world water chemistry. *Science* 170(3962):1088–1090. <https://doi.org/10.1126/science.170.3962.1088>
- Gopinath S, Srinivasamoorthy K, Saravanan K, Suma CS, Prakash R, Senthinathan D, Sarma VS (2017) Vertical electrical sounding for mapping saline water intrusion in coastal aquifers of Nagapattinam and Karaikal, South India. *Sustain Water Resour Manag* 4(4):833–841. <https://doi.org/10.1007/s40899-017-0178-4>
- Gopinath S, Srinivasamoorthy K, Prakash R, Saravanan K, Karunanidhi D (2019) Hydrogeochemistry of groundwater From Tamil Nadu and Pondicherry Coastal Aquifers, South India: implication for chemical characteristics and sea water intrusion. *GIS Geostat Techn Groundwater Sci*:237–249. <https://doi.org/10.1016/b978-0-12-815413-7.00017-1>
- Halim MA, Majumder RK, Nessa SA, Hiroshiro Y, Sasaki K, Saha BB, Jinno K (2010) Evaluation of processes controlling the geochemical constituents in deep groundwater in Bangladesh: spatial variability on arsenic and boron enrichment. *J Hazard Mater* 180(1–3):50–62. <https://doi.org/10.1016/j.jhazmat.2010.01.008>
- Handa BK (1988) Content of potassium in groundwater in India. *Fertil News* 33(11):15–27
- Jabal MSA, Abustan I, Rozaimy MR, El Najar H (2014) Groundwater beneath the urban area of Khan Younis City, southern Gaza Strip (Palestine): hydrochemistry and water quality. *Arab J Geosci* 8(4): 2203–2215. <https://doi.org/10.1007/s12517-014-1346-6>
- Jain CK, Bandyopadhyay A, Bhadra A (2009) Assessment of groundwater quality for drinking purposes, District Nainital, Uttarakhand, India. *Environ Monit Assess* 166(1–4):663–676. <https://doi.org/10.1007/s10661-009-1031-5>
- Jayakumar R, Siraz L (1997) Factor analysis in hydrogeochemistry of coastal aquifers - a preliminary study. *Environ Geol* 31(3–4):174–177. <https://doi.org/10.1007/s002540050177>
- Karanth KR (1989) *Groundwater assessment development and management*. Tata McGraw-Hill Publ. Com. Ltd, New Delhi
- Kattan Z (2018) Using hydrochemistry and environmental isotopes in the assessment of groundwater quality in the Euphrates alluvial aquifer, Syria. *Environ Earth Sci* 77(2). <https://doi.org/10.1007/s12665-017-7197-1>
- Khan AF, Srinivasamoorthy K, Rabina C (2020) Hydrochemical characteristics and quality assessment of groundwater along the coastal tracts of Tamil Nadu and Puducherry, India. *Appl Water Sci* 10(2). <https://doi.org/10.1007/s13201-020-1158-7>
- Kortatsi BK, Tay CK, Anornu G, Hayford E, Dartey GA (2007) Hydrogeochemical evaluation of groundwater in the lower Offin basin, Ghana. *Environ Geol* 53(8):1651–1662. <https://doi.org/10.1007/s00254-007-0772-0>
- Lee JY, Choi JC, Yi MJ, Kim JW, Cheon JY, Choi YK, Lee KK (2005) Potential groundwater contamination with toxic metals in and around an abandoned Zn mine, Korea. *Water Air Soil Pollut* 165(1–4):167–185. <https://doi.org/10.1007/s11270-005-4637-4>
- Li P, Qian H, and Wu J. 2010. Groundwater quality assessment based on improved water quality index in Pengyang County, Ningxia, northwest China. *E-J Chem* 7(S1):S209–S216. <https://doi.org/10.1155/2010/451304>
- Manjusree TM, Joseph S, Petitta M, Thomas J (2017) Integrated approach for identifying the factors controlling groundwater quality of a tropical coastal zone in Kerala, India. *Environ Earth Sci* 76(14). <https://doi.org/10.1007/s12665-017-6818-z>
- Mantelin S, Touraine B (2004) Plant growth-promoting bacteria and nitrate availability. Impacts on root development and nitrate uptake. *J Exp Bot*. <https://doi.org/10.1093/jxb/erh010>
- Mapoma HWT, Xie X, Liu Y, Zhu Y, Kawaye FP, Kayira TM (2017) Hydrochemistry and quality of groundwater in alluvial aquifer of Karonga, Malawi. *Environmental Earth Sciences*, 76(9). <https://doi.org/10.1007/s12665-017-6653-2>
- Matthess G (1982) *The properties of groundwater*. Wiley, New York, p 498
- Meadows DG, Caballero JP, Kruse SE, Vacher HL (2004) Variation of salinity in brackish-water lenses of two Florida keys. *J Coast Res* 202:386–400. [https://doi.org/10.2112/1551-5036\(2004\)020\[0386:vosibl\]2.0.co;2](https://doi.org/10.2112/1551-5036(2004)020[0386:vosibl]2.0.co;2)
- Meybeck M (1987) Global chemical weathering of surficial rocks estimated from river dissolved loads. *Am J Sci* 287(5):401–428. <https://doi.org/10.2475/ajs.287.5.401>
- Moncaster S, Bottrell S, Tellam J, Lloyd J, Konhauser K (2000) Migration and attenuation of agrochemical pollutants: insights from isotopic analysis of groundwater sulphate. *J Con-tam Hydrol* 43(2): 147–163. [https://doi.org/10.1016/s0169-7722\(99\)00104-7](https://doi.org/10.1016/s0169-7722(99)00104-7)
- Mondal NC, Singh VP, Singh S, Singh VS (2010a) Hydrochemical characteristics of the coastal aquifer from Tuticorin, Tamil Nadu, India. *Environ Monit Assess* 175(1–4):531–550. <https://doi.org/10.1007/s10661-010-1549-6>
- Mondal NC, Singh VS, Saxena VK, Singh VP (2010b) Assessment of seawater impact using major hydrochemical ions: a case study from Sadras, Tamilnadu, India. *Environ Monit Assess* 177(1–4):315–335. <https://doi.org/10.1007/s10661-010-1636-8>
- Monjerezi M, Ngongondo C (2012) Quality of groundwater resources in Chikhwawa, Lower Shire Valley, Malawi. *Water Qual Expo Health* 4(1):39–53. <https://doi.org/10.1007/s12403-012-0064-0>
- Morris BL, Lawrence ARL, Chilton PJC, Adams B, Calow RC, Klinck BA (2003) Groundwater and its susceptibility to degradation global assessment of the problem and options for management. Early warning and assessment report series, RS. 03–3, United Nations Environment Programme, Nairobi, Kenya
- Mukherjee A, Fryar AE (2008) Deeper groundwater chemistry and geochemical modeling of the arsenic affected western Bengal basin, West Bengal, India. *Appl Geochem* 23(4):863–894. <https://doi.org/10.1016/j.apgeochem.2007.07.011>
- Nkotagu H (1996) The groundwater geochemistry in a semi-arid, fractured crystalline basement area of Dodoma, Tanzania. *J Afr Earth Sci* 23(4):593–605

- Obeidatt A, Alawneh M (2019) Hydrochemistry and Groundwater Quality Assessment in Mafraq Province, Jordan. *OALib*, 06(04), 1–10. <https://doi.org/10.4236/oalib.1105365>
- Piper AM (1944) A graphic procedure in the geochemical interpretation of water analyses. *Trans Am Geophys Union* 25(6):914. <https://doi.org/10.1029/tr025i006p00914>
- Playán E, Mateos L (2006) Modernization and optimization of irrigation systems to increase water productivity. *Agric Water Manag* 80(1-3): 100–116. <https://doi.org/10.1016/j.agwat.2005.07.007>
- Rajmohan N, Elango L (2003) Identification and evolution of hydrogeochemical processes in the groundwater environment in an area of the Palar and Cheyyar River Basins, Southern India. *Environ Geol* 1(1): 1. <https://doi.org/10.1007/s00254-004-1012-5>
- Rogers RJ (1989) Geochemical comparison of ground water in areas of New England, New York, and Pennsylvania. *Ground Water* 27(5): 690–712. <https://doi.org/10.1111/j.1745-6584.1989.tb00483.x>
- Sajil Kumar PJ (2016) Deciphering the groundwater–saline water interaction in a complex coastal aquifer in South India using statistical and hydrochemical mixing models. *Model Earth Syst Environ* 2(4): 1–11. <https://doi.org/10.1007/s40808-016-0251-2>
- Sako A, Yaro JM, Bamba O (2018) Impacts of hydrogeochemical processes and anthropogenic activities on groundwater quality in the Upper Precambrian sedimentary aquifer of northwestern Burkina Faso. *Appl Water Sci* 8(3). <https://doi.org/10.1007/s13201-018-0735-5>
- Schoeller H (1965) Qualitative evaluation of groundwater resources. In: *Methods and techniques of groundwater investigations and developments*, UNESCO, pp 54–83
- Schoeller H (1977) *Geochemistry of groundwater*. In *groundwater studies—an international guide for research and practice* (Ch. 15, pp. 1–18). Paris:UNESCO.
- Schuh WM, Klinkebiel DL, Gardner JC, Meyer RF (1997) Tracer and nitrate movement to groundwater in the Northern Great Plains. *J Environ Qual* 26(5):1335–1347. <https://doi.org/10.2134/jeq1997.00472425002600050020x>
- Song SH, Lee JY, Park N (2007) Use of vertical electrical soundings to delineate seawater intrusion in a coastal area of Byunsan, Korea. *Environ Geol* 52:1207–1219
- Srinivasamoorthy K, Chidambaram S, Prasanna MV, Vasanthavihar M, Peter J, Anandhan P (2008) Identification of major sources controlling groundwater chemistry from a hard rock terrain — a case study from Mettur taluk, Salem district, Tamil Nadu, India. *J Earth Syst Sci* 117(1):49–58. <https://doi.org/10.1007/s12040-008-0012-3>
- Srinivasamoorthy K, Vasanthavigar M, Vijayaraghavan K, Sarathidasan R, Gopinath S (2011) Hydrochemistry of groundwater in a coastal region of Cuddalore district, Tamilnadu, India: implication for quality assessment. *Arab J Geosci* 6(2):441–454. <https://doi.org/10.1007/s12517-011-0351-2>
- Srinivasamoorthy K, Vasanthavigar M, Vijayaraghavan K, Sarathidasan R, Gopinath S (2013) Hydrochemistry of groundwater in a coastal region of Cuddalore district, Tamilnadu, India: implication for quality assessment. *Arabian Journal of Geosciences* 6 (2):441–454
- Srinivasamoorthy K, Gopinath M, Chidambaram S, Vasanthavigar M, Sarma VS (2014) Hydrochemical characterization and quality appraisal of groundwater from Pungar sub-basin, Tamilnadu, India. *J King Saud Univ - Sci* 26(1):37–52. <https://doi.org/10.1016/j.jksus.2013.08.001>
- Subba Rao, N. (2008). Factors controlling the salinity in groundwater in parts of Guntur district, Andhra Pradesh, India. *Environmental Monitoring and Assessment* 138 (1-3):327–341
- Subrahmanyam K, Yadaiah P (2001) Assessment of the impact of industrial effluents on water quality in Patancheru and environs, Medak district, Andhra Pradesh, India. *Hydrogeol J* 9(3):297–312. <https://doi.org/10.1007/s100400000120>
- Sunitha V, Sudharshan Reddy Y (2019) Hydrogeochemical evaluation of groundwater in and around Lakkireddipalli and Ramapuram, Y.S.R District, Andhra Pradesh, India. *HydroResearch* 2:85–96. <https://doi.org/10.1016/j.hydres.2019.11.008>
- Vasanthavigar M, Srinivasamoorthy K, Prasanna MV (2012) Identification of groundwater contamination zones and its sources by using multivariate statistical approach in Thirumanimuthar sub-basin, Tamil Nadu, India. *Environ Earth Sci* 68(6):1783–1795. <https://doi.org/10.1007/s12665-012-1868-8>
- Wen X, Wu Y, Su J, Zhang Y, Liu F (2005) Hydrochemical characteristics and salinity of groundwater in the Ejina Basin, Northwestern China. *Environ Geol* 48(6):665–675. <https://doi.org/10.1007/s00254-005-0001-7>
- Wirmvem MJ, Ohba T, Suila JY, Fantong WY, Bate NO, Ooki S, Wotany ER, Asaah ANE, Ayonghe SN, Tanyileke G, Hell JV (2014) Hydrochemical and isotopic characteristics of groundwater in the Ndop plain, northwest Cameroon: resilience to seasonal climatic changes. *Environ Earth Sci* 72(9):3585–3598. <https://doi.org/10.1007/s12665-014-3265-y>
- Yidana SM (2010) Groundwater classification using multivariate statistical methods: Southern Ghana. *J Afr Earth Sci* 57(5):455–469. <https://doi.org/10.1016/j.jafrearsci.2009.12.002>
- Zaidi FK, Nazzal Y, Jafri MK, Naeem M, Ahmed I (2015) Reverse ion exchange as a major process controlling the groundwater chemistry in an arid environment: a case study from northwestern Saudi Arabia. *Environ Monit Assess* 187(10):607. <https://doi.org/10.1007/s10661-015-4828-4>

Publisher's note Springer Nature remains neutral with regard to jurisdictional claims in published maps and institutional affiliations.